

國立臺灣大學公共衛生學院環境與職業健康科學研究所



碩士論文

Institute of Environmental and Occupational Health Sciences

Department of Public Health

National Taiwan University

Master Thesis

大台北地區自來水系統清水及水源中含鈦奈米微粒調查

Investigation of Ti-containing Nanoparticles in Finished Water and  
the Water Sources of the Drinking Water System in the Greater  
Taipei Area

陳柔安

Jou-An Chen

指導教授：黃耀輝 博士

Advisor: Yaw-Huei Huang, Ph.D.

中華民國 110 年 1 月

January, 2021

## 中文摘要



奈米科技迅速發展，人工奈米物質在生活中的應用日益增加，這些奈米物質可能隨著人類活動釋放到環境，成為環境中的新興污染物。當奈米微粒進入飲用水水源，人們便可能通過飲用水攝入人工奈米微粒，進一步可能造成氧化壓力、發炎反應以及細胞凋亡等健康方面不良影響。

本研究對大台北地區主要河川水源與飲用水系統中含奈米微粒分佈進行調查，包含淡水河流域基隆河、新店溪與大漢溪等三大支流河川水源，以及大台北地區五座負責主要供水的淨水場飲用水系統樣本。使用單粒子感應耦合電漿質譜儀 (single-particle inductively coupled plasma-mass spectrometry) 分析樣本當中含鈦奈米微粒質量濃度 (ng/mL)、數目濃度 ( $\times 10^3$  part./mL) 與粒徑分佈 (nm)。

分析結果顯示含鈦微粒濃度在河川中呈現出各河川之間的區域性差異及明顯的季節性變化趨勢，推測受區域的地質以及土地利用影響。質量濃度的整體範圍在基隆河、新店溪、大漢溪分別為 1.14–11.5 ng/mL、0.05–1.92 ng/mL 和 0.72–12.2 ng/mL。數目濃度的整體範圍在基隆河、新店溪、大漢溪分別為  $170\text{--}4,109 \times 10^3$  part./mL、 $5.32\text{--}417 \times 10^3$  part./mL 和  $108\text{--}4,162 \times 10^3$  part./mL。含鈦微粒以 100 nm 以下的奈米級微粒為多數，最常見粒徑在基隆河的範圍為 36–42 nm、在新店溪為 38–66 nm 以及在大漢溪為 38–76 nm。

此外，傳統淨水處理移除含鈦微粒的效率約在 83% 到 99% 之間，最終清水中存在的含鈦微粒的質量濃度、數目濃度與粒徑範圍依序為 0.01–0.40 ng/mL、 $0.41\text{--}260 \times 10^3$  part./mL 以及 42–52 nm。

關鍵字：二氧化鈦、奈米微粒、地表水、飲用水、單粒子感應耦合電漿質譜儀

## ABSTRACT



The application of engineered nanomaterials in daily life is increasing. These nanomaterials may be released into the environment with human activities and become emerging pollutants in the environment. When nanoparticles enter drinking water sources, people may ingest engineered nanoparticles through drinking water, which may further cause adverse health effects such as oxidative stress, inflammation, and apoptosis.

This study investigated the distribution of Ti-containing nanoparticles in major river water sources and drinking water systems in the Greater Taipei area, including the Keelung River, Xindian River, and Dahan River, as well as samples of drinking water systems in the five major water treatment plants in the Greater Taipei Area. Single-particle inductively coupled plasma-mass spectrometry was used to analyze the mass concentration (ng/mL), particle concentration ( $\times 10^3$  part./mL), and particle size distribution of Ti-containing nanoparticles in the sample (nm).

The analysis results show that the concentration of Ti-containing particles in rivers presents regional differences and obvious seasonal changes, which may be the result of the influence of regional geology and land use. The mass concentration ranges of Ti-containing particles in the Keelung River, Xindian River and Dahan River were 1.14–11.5 ng/mL, 0.05–1.92 ng/mL and 0.72–12.2 ng/mL, respectively. For the number concentration, the overall ranges in the Keelung River, Xindian River and Dahan River were  $170\text{--}4,109 \times 10^3$  parts/ml,  $5.32\text{--}417 \times 10^3$  parts/ml and  $108\text{--}4,162 \times 10^3$  parts/ml. Most of the measured Ti-containing particles were smaller than 100 nm, and the most frequent size ranges were 36–42 nm in the Keelung River, 38–66 nm in the Xindian River, and 38–76 nm in the Dahan River.

This study also confirmed that conventional water treatment can effectively remove Ti-containing particles from raw water, with a removal efficiency of about 83% to 99%. The mass concentration, number concentration and most frequent size ranges of the Ti-containing particles remaining in the finished water were 0.01–0.40 ng/mL, 0.41–260 ×10<sup>3</sup> parts/mL and 42–52 nm, respectively.

Key words: titanium dioxide, nanoparticle, surface water, drinking water, single-particle inductively coupled plasma mass spectrometry

# CONTENTS



中文摘要 .....	i
ABSTRACT .....	ii
CONTENTS .....	iv
LIST OF FIGURES .....	vii
LIST OF TABLES .....	ix
<b>Chapter 1 Introduction .....</b>	<b>1</b>
1.1 Background.....	1
1.2 Study Aims .....	2
<b>Chapter 2 Literature Review .....</b>	<b>3</b>
2.1 Definition and classification of nanoparticles .....	3
2.1.1 Definition .....	3
2.1.2 Classification.....	3
2.2 Pathways of engineered nanoparticles entering the environment.....	5
2.3 The concentrations of metal ENPs in surface water and tap water .....	6
2.4 Removal of nanoparticles through conventional water treatment .....	10
2.5 Toxicity of TiO <sub>2</sub> nanoparticles.....	11
<b>Chapter 3 Materials and Methods.....</b>	<b>14</b>
3.1 Water Sample Collection .....	14
3.1.1 Materials and equipment .....	14
3.1.2 Sampling Sites.....	14
3.1.3 Sampling procedure.....	20
3.2 Ti-containing nanoparticles analysis .....	22



3.2.1	Standards, chemicals, and materials.....	22
3.2.2	Sample pretreatment.....	22
3.2.3	Preparation of Calibration Curves.....	23
3.2.4	Instrumental Analysis.....	24
3.2.5	Detection Limits.....	25
3.2.6	QA/QC .....	26
<b>Chapter 4</b>	<b>Results .....</b>	<b>27</b>
4.1	Distribution of Ti-containing nanoparticles in drinking water sources .....	27
4.1.1	Keelung River .....	27
4.1.2	Xindian River and its upstream tributaries.....	34
4.1.3	Dahan River and its tributary .....	44
4.2	Distribution of Ti-containing nanoparticles in drinking water systems.....	52
4.2.1	Drinking water from the Keelung River .....	52
4.2.2	Drinking water from the Xindian River .....	55
4.2.3	Drinking water from the Dahan River and its tributary .....	58
<b>Chapter 5</b>	<b>Discussion.....</b>	<b>68</b>
5.1	Detection of Ti containing particles in the water sources of the Greater Taipei area.....	68
5.1.1	Comparison with previous studies in mass concentration, number concentration, and particle size .....	68
5.1.2	Spatial distribution of mass concentration and possible origins of the Ti-containing particles.....	70
5.1.3	Seasonal changes, possible causes, in mass concentration .....	74
5.1.4	Possible factors affecting particle sizes.....	77
5.2	Ti-containing particles in drinking water.....	79

**Chapter 6 Conclusions.....83**

REFERENCES .....85



# LIST OF FIGURES



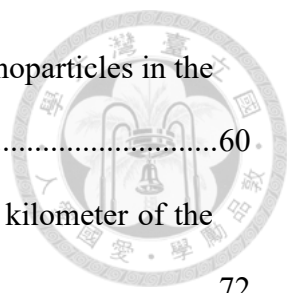
Fig. 3-1	Map of the Keelung River and sampling sites listed in table 3-1.....	16
Fig. 3-2	Map of the Xindian River, Beishi River, Nanshi River, and sampling locations listed in table 3-2.....	18
Fig. 3-3	Map of the Dahan River, Sanxia River, and sampling locations listed in table 3-3. ....	20
Fig. 4-1	Total Ti and particle Ti mass concentration (a,d), number concentration (b,e), and the most frequent size (c,f) of Ti-containing nanoparticles in the Keelung River. ....	30
Fig. 4-2	Total Ti and particle Ti mass concentration (a,d), number concentration (b,e), and the most frequent size (c,f) of Ti-containing nanoparticles in the Xindian River and its upstream tributaries. ....	37
Fig. 4-3	Total Ti and particle Ti mass concentration (a,d), number concentration (b,e), and the most frequent size (c,f) of Ti-containing nanoparticles in the Dahan River and its tributary. ....	47
Fig. 4-4	Total Ti and particle Ti mass concentration (a,d), number concentration (b,e), and the most frequent size (c,f) of Ti-containing nanoparticles in raw water and finished water from the Xinshan WTP. ....	54
Fig. 4-5	Total Ti and particle Ti mass concentration (a,d), number concentration (b,e), and the most frequent size (c,f) of Ti-containing nanoparticles in the raw water and finished water from the Zhitan, Changxing, and Gongguan WTP. ....	57
Fig. 4-6	Total Ti and particle Ti mass concentration (a,d), number concentration	

(b,e), and the most frequent size (c,f) of Ti-containing nanoparticles in the raw water and finished water from the Bansin WTP. ....60

Fig. 5-1 Map of built-up land use of the riparian area within one kilometer of the Keelung River, Xindian River, and Dahan River.....72

Fig. 5-2 Map of the sampling site downstream from the sewage treatment outfall...74

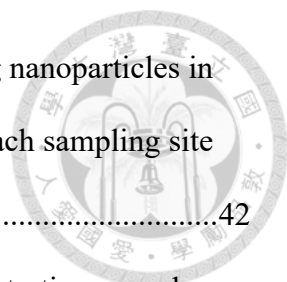
Fig. 5-3 Proportion of Ti in the form of particle by percentage (%) and turbidity (NTU) in samples from (a) Keelung River, (b) Xindian River, and (c) Dahan River, respectively, in both dry and wet season. ....76



# LIST OF TABLES



Table 2-1. Concentrations of common metallic nanoparticles in surface water and tap water reported in previous studies. ....	8
Table 3-1. Coordinates of sampling sites of the Keelung River tap water intake and supply system.....	15
Table 3-2. Coordinates of sampling sites of the Xindian River tap water intake and supply system.....	17
Table 3-3. Coordinates of sampling sites of the Dahan River tap water intake and supply system.....	19
Table 3-4. Single particle acquisition mode operating parameters for sp-ICPMS. ....	24
Table 4-1. Total Ti mass concentration, particle Ti mass concentration, number concentration and the most frequent size of Ti-containing nanoparticles in the Keelung River. ....	31
Table 4-2. Water quality measurements of the Keelung River. ....	32
Table 4-3. Total Ti mass concentration, particle Ti mass concentration, number concentration and the most frequent size of Ti-containing nanoparticles in transport blank and field blank samples collected from each sampling site of the Keelung River. ....	33
Table 4-4. Total Ti mass concentration, particle Ti mass concentration, number concentration and the most frequent size of Ti-containing nanoparticles in the Xindian River, Beishi River and Nanshi River. ....	38
Table 4-5. Water quality measurements of the Xindian River and its tributaries. ....	40
Table 4-6. Total Ti mass concentration, particle Ti mass concentration, number	



concentration and the most frequent size of Ti-containing nanoparticles in transport blank and field blank samples collected from each sampling site of the Xindian River and its tributaries.....42

Table 4-7. Total Ti mass concentration, particle Ti mass concentration, number concentration and the most frequent size of Ti-containing nanoparticles in the Dahan River and its tributary. ....48

Table 4-8. Water quality measurements of the Dahan River.....50

Table 4-9. Total Ti mass concentration, particle Ti mass concentration, number concentration and the most frequent size of Ti-containing nanoparticles in transport blank and field blank samples collected from each sampling site of the Dahan River and its tributary.....51

Table 4-10. Total Ti mass concentration, particle Ti mass concentration, number concentration and the most frequent size of Ti-containing nanoparticles in raw water and finished water. ....61

Table 4-11. Water quality parameters of raw water and finished water.....64

Table 4-12. Total Ti mass concentration, particle Ti mass concentration, number concentration and the most frequent size of Ti-containing nanoparticles in water treatment plant field blanks.....66

Table 5-1. The total Ti mass concentration, particle Ti mass concentration, number concentration and most frequent size of the Ti-containing particles in the river water samples downstream of the sewage treatment outfall. ....73

# Chapter 1 Introduction



## 1.1 Background

In recent years, engineered nanomaterials have been widely used in industry as well as in the manufacturing of consumer products. These nanomaterials, mostly metallic nanoparticles, may be released into the environment during the production, use, and disposal of products (Gottschalk *et al.*, 2013) and thus become emerging pollutants in the environment, which exposes the environment and organisms to potential risks (Moore, 2006).

Nanoparticles released into the water bodies may inevitably enter drinking water sources. Since the current conventional water treatment process cannot wholly remove nanoparticles from raw water (Chalew *et al.*, 2013), tap water has become one of the ways for humans to be exposed to nanoparticles. Although the effect on humans is still unclear, the adverse health effects from exposure to nanoparticles have been observed in animal and in vitro experiments (von Moos and Slaveykova, 2014).

Previous research has indicated that the production of nano-TiO<sub>2</sub> worldwide reached 100,000 megagrams per year in 2015, and 72% was used in the manufacturing of personal care products (Jankovic and Plata, 2019). Compared with other nanomaterials on the market, nano-TiO<sub>2</sub> is widely used in products with high usage and high popularity, and has characteristics of high production volume, so it is more likely to enter the water bodies through domestic wastewater. Since nano-TiO<sub>2</sub> may be the most commonly released engineered nanomaterial in the environment, the potential impact on the environment and human health cannot be overlooked (Gottschalk and Nowack, 2011).

The release of nanoparticles into surface water has raised concerns about the

ingestion of engineered nanoparticles through drinking water and the food chain (Tiede *et al.*, 2016). In order to conduct an in-depth risk assessment of nanoparticles, the inherent hazards of nanoparticles and the possibility of exposure to nanoparticles are quite crucial. Thus, it is necessary to understand further the characteristics and concentration of nanoparticles in the environment to ensure population health and safety.

## 1.2 Study Aims

In this study, the Ti-containing nanoparticle was selected as the research object. We obtained mass concentration, number concentration, and particle size information by using single particle inductively coupled plasma mass spectrometry (sp-ICPMS). The analysis results were used to (1) establish the characteristics and distribution information of Ti-containing nanoparticles in drinking water and river water sources in the Greater Taipei area, and to (2) evaluate the Ti-containing nanoparticle removal efficiency of the current water treatment. Also, this study discusses factors that may determine the characteristics and distribution of Ti-containing nanoparticles.

## Chapter 2 Literature Review



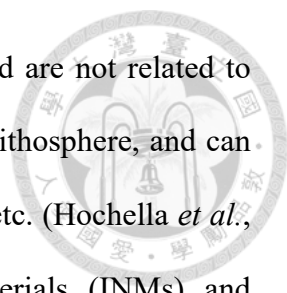
### 2.1 Definition and classification of nanoparticles

#### 2.1.1 Definition

The definition of nanoparticles has been proposed by many organizations, commonly defined by size, with the diameter ranging from 1 to 100 nm. The International Organization for Standardization (ISO) defines substances with at least one dimension in the size range of 1 nm to 100 nm as nanomaterials, and if all dimensions are at the nanoscale, they are classified as nanoparticles (ISO, 2015). According to the definition proposed by the British Standards Institution, materials with any internal or external structure at the nanoscale are defined as nanomaterials, and nanoobjects with three external nanoscale dimensions are defined as nanoparticles (BSI, 2011). The European Commission provides recommendations that nanomaterials are composed of particles and that 50% or more of the particles have at least one dimension ranging from 1 nm to 100 nm (EU, 2011). Since nanoscale particles exhibit distinct general properties, nanoparticles can also be defined according to characteristics. Study has suggested that when particles exhibit different physicochemical and biological properties compared to bulk materials, the particle size is defined to be within the nanoscale range of the specific material. Accordingly, the nanoscale range of metallic nanoparticles is about  $\leq 30$  nm (Auffan *et al.*, 2009).

#### 2.1.2 Classification

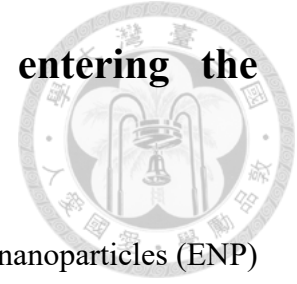
Nanomaterials can be classified based on origins, including natural nanomaterials and anthropogenic nanomaterials (Hochella *et al.*, 2019). Natural nanomaterials (NNMs)



are naturally produced by geochemical or mechanical processes and are not related to human activities. NNMs exist in the atmosphere, hydrosphere and lithosphere, and can be found in oceans, lakes, rivers, groundwater, rocks, soil, magma, etc. (Hochella *et al.*, 2015). Anthropogenic nanomaterials include incidental nanomaterials (INMs) and engineered nanomaterials (ENMs). INMs are by-products that are inadvertently produced during human activities, such as by mechanical grinding, combustion, and fuel exhaust. ENMs are designed by humans and intentionally produced, providing select physical or chemical properties for specific applications, including advanced materials, electronics, cosmetics, medical drug design and many other fields (Jankovic and Plata, 2019; Piccinno *et al.*, 2012). A study predicted that the compound annual growth rate of ENM production in the European market from 2016 to 2022 is 20.0%, confirming the rapid growth of ENMs production (Inshakova and Inshakov, 2017). Therefore, it is necessary to investigate the possible impact of ENMs on the environment and organisms.

Nanomaterials can also be classified into carbon-based, inorganic-based, organic-based, and composite materials based on material composition (Jeevanandam *et al.*, 2018). Examples of carbon-based nanomaterials are fullerene (C<sub>60</sub>), carbon nanotubes (CNT), and graphene. Organic-based nanomaterials are mainly made of organic substances, such as dendrimers, liposomes, micelles, and polymers, but do not include carbon-based nanomaterials. Inorganic-based nanomaterials include metals (e.g., Au and Ag), metal oxides (e.g., TiO<sub>2</sub>, SiO<sub>2</sub>, FeO<sub>x</sub>, AlO<sub>x</sub>, and ZnO), as well as semiconductors (e.g., silicon and ceramics). Composite nanomaterials are the combination of different types of nanomaterials or the combination of nanomaterials to bulk materials. All types of nanomaterials can be found in NNMs. As for ENMs, inorganic-based and carbon-based materials are mainly manufactured and applied in the current market (Jankovic and Plata, 2019; Piccinno *et al.*, 2012).

## 2.2 Pathways of engineered nanoparticles entering the environment



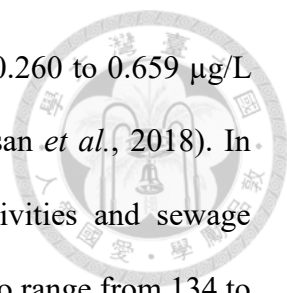
In recent years, the application and manufacture of engineered nanoparticles (ENP) have increased significantly, thus raising interests about the possible entry of ENP into the environment. Studies have indicated that the increase in production volume of ENPs and the wide application of products will lead to diversified emission pathways (Nowack and Bucheli, 2007). ENPs are usually released directly into the environment along the life cycle of their products in the following conditions: (1) emissions or leakage from industrial facilities in the production of raw materials and products (Benn and Westerhoff, 2008; Johnson and Park, 2012); (2) released during use of the products (Gondikas *et al.*, 2014; Kaegi *et al.*, 2008); (3) released at the disposal stage of products containing ENPs (Keller *et al.*, 2013). Also, ENPs may also be discharged indirectly through technical facilities such as wastewater treatment plants or landfills (Kaegi *et al.*, 2010; Kaegi *et al.*, 2011).

The emission pathway is determined by the nature and application of ENPs. For example, TiO<sub>2</sub> is a white pigment commonly found in paints, paper, plastics, ceramics, food additives, and is used in the manufacture of sunscreens, toothpastes, pharmaceuticals, and cosmetics due to its UV resistant and photocatalytic properties (Weir *et al.*, 2012). Because it is widely used in the manufacture of cosmetics and consumer products, the dominant discharge pathway of TiO<sub>2</sub> ENPs is via domestic wastewater, accounting for 85% of the total discharge (Keller *et al.*, 2013). Nanoparticles are often still present in the wastewater effluent after conventional treatment (Westerhoff *et al.*, 2011) and then can be released into surface water. In addition, ENPs accumulate in wastewater sludge during the wastewater treatment process and may eventually be used as agricultural fertilizers or

in horticultural applications, which will release ENPs to the soil or transported to surface water through agricultural runoff (Keller *et al.*, 2013; Mahdi *et al.*, 2017; Mueller and Nowack, 2008). When the use of outdoor applications (e.g., architectural paints) increases, the mass flow of nanoparticles entering aquatic and terrestrial environments therefore increases, and similar association for engineered TiO<sub>2</sub> nanoparticles has also been confirmed in other studies (Baalousha *et al.*, 2016; Bossa *et al.*, 2017).

### **2.3 The concentrations of metal ENPs in surface water and tap water**

Based on the material flow analysis, it is estimated that the probability of ENMs appearing in the surface water is in proportion to the global production level (Keller and Lazareva, 2014). Therefore, TiO<sub>2</sub> is one of the nanomaterials most likely to appear in water sources and drinking water systems (Westerhoff *et al.*, 2018). In recent years, sp-ICPMS technology made it achievable to quantify nanoparticles in environmental water samples with low predicted concentrations ranging from ppt to low ppb. Peters *et al.* analyzed the real river water samples in the Netherlands and found that the concentration of nanoparticles detected in the surface water was consistent with the environmental concentration predicted by the MFA model, where the mass concentration and number concentration of TiO<sub>2</sub> particles were 0.2–8.1 µg/L and 5–150 ×10<sup>3</sup> part./mL, respectively (Peters *et al.*, 2018). In South Africa, the concentration of Ti-containing nanoparticles measured in freshwater dams was 83–140 ×10<sup>3</sup> part./mL (Maiga *et al.*, 2019). Gondikas *et al.* measured the mass concentration of Ti-containing particles to be 1.38 µg/L in the Old Danube Lake in Austria as a recreational water area, which may receive engineered TiO<sub>2</sub> released from sunscreen (Gondikas *et al.*, 2014). Another similar study found that



the mass concentration of Ti-containing nanoparticles ranged from 0.260 to 0.659  $\mu\text{g/L}$  in the bathing area of the Salt River in the United States (Venkatesan *et al.*, 2018). In France, the Loire River, which is affected by anthropogenic activities and sewage discharge, the concentration of Ti-containing particles was reported to range from 134 to  $803 \times 10^3$  part./mL. According to an investigation of river water, tap water and sewage treatment plant effluents, the lowest concentration of  $\text{TiO}_2$  nanoparticles detected in tap water was 3.1 ng / L, while the concentration of river water and sewage treatment effluent samples ranged from 57 to 895 ng / L (Yang and Westerhoff, 2014). Donovan *et al.* also reported the concentration of Ti-containing particles in river water and drinking water samples, expressed in number concentration as  $425\text{--}451 \times 10^3$  part./mL and  $15\text{--}17 \times 10^3$  part./mL, respectively (Donovan *et al.*, 2016). These studies confirmed that Ti-containing nanoparticles are present in rivers, tap water, and sewage, and that consumers may be exposed to low concentrations of engineered  $\text{TiO}_2$  from drinking water.

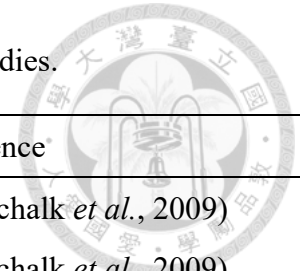


Table 2-1. Concentrations of common metallic nanoparticles in surface water and tap water reported in previous studies.

Nanoparticles	Method	Research Area	Surface Water	Tap Water	Reference
TiO <sub>2</sub>	Modeling	Europe	0.012–0.057 µg/L	–	(Gottschalk <i>et al.</i> , 2009)
	Modeling	US	0.002–0.010 µg/L	–	(Gottschalk <i>et al.</i> , 2009)
	Modeling	Europe	0.4–1.4 µg/L	–	(Sun <i>et al.</i> , 2014)
	Modeling	UK	4.91–164 µg/L	0.05–1.64 µg/L	(Tiede <i>et al.</i> , 2016)
	ICPMS	England	0.94–1.81 µg/L	–	(Neal <i>et al.</i> , 2011)
	sp-ICPMS	US	0.895 µg/L	0.003 µg/L	(Yang and Westerhoff, 2014)
	sp-ICPMS	Austria	1.38 µg/L	–	(Gondikas <i>et al.</i> , 2014)
	sp-ICPMS	US	425–451 ×10 <sup>3</sup> part./mL	15–17 ×10 <sup>3</sup> part./mL	(Donovan <i>et al.</i> , 2016)
	sp-ICPMS	Netherlands	0.2–8.1 µg/L 5–150 ×10 <sup>3</sup> part./mL	–	(Peters <i>et al.</i> , 2018)
	sp-ICPMS	US	0.260–0.659 µg/L	–	(Venkatesan <i>et al.</i> , 2018)
	Sp-ICPMS	South Africa	83–140 ×10 <sup>3</sup> part./mL	–	(Maiga <i>et al.</i> , 2019)
	Sp-ICPMS	France	134–803 ×10 <sup>3</sup> part./mL	–	(Phalyvong <i>et al.</i> , 2020)

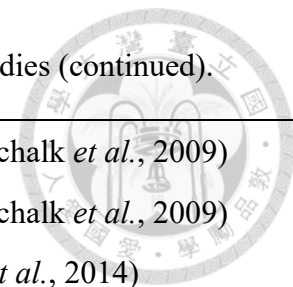
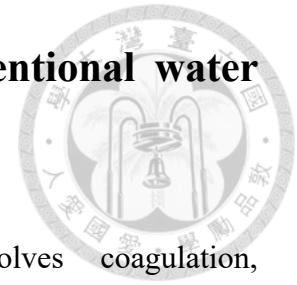


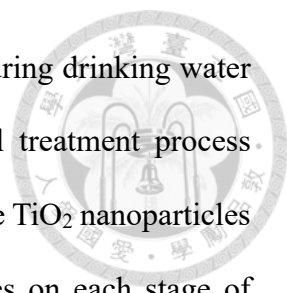
Table 2-1. Concentrations of common metallic nanoparticles in surface water and tap water reported in previous studies (continued).

ZnO	Modeling	Europe	0.008–0.055 µg/L	–	(Gottschalk <i>et al.</i> , 2009)
	Modeling	US	0.001–0.003 µg/L	–	(Gottschalk <i>et al.</i> , 2009)
	Modeling	Europe	1.7–21 µg/L	–	(Sun <i>et al.</i> , 2014)
	Modeling	UK	1.91–63.6 µg/L	0.02–0.64 µg/L	(Tiede <i>et al.</i> , 2016)
SiO <sub>2</sub>	Modeling	Europe	0.00–25.5 µg/L	–	(Giese <i>et al.</i> , 2018)
Ag	Modeling	Europe	0.59–2.16 µg/L	–	(Gottschalk <i>et al.</i> , 2009)
	Modeling	US	0.09–0.43 µg/L	–	(Gottschalk <i>et al.</i> , 2009)
	Modeling	Europe	0.51–0.94 µg/L	–	(Sun <i>et al.</i> , 2014)
	Modeling	Europe	0.00–4.17 µg/L	–	(Giese <i>et al.</i> , 2018)
	Modeling	UK	0.32–10.7 µg/L	0.003–0.10 µg/L	(Tiede <i>et al.</i> , 2016)
	sp-ICPMS	US	0.2 ng/L	1.9 ng/L	(Yang and Westerhoff, 2014)
	sp-ICPMS	Netherlands	0.3–2.5 ng/L	–	(Peters <i>et al.</i> , 2018)
CeO <sub>2</sub>	Modeling	Europe	0.00–61.74 µg/L	–	(Giese <i>et al.</i> , 2018)
	sp-ICPMS	US	18 ng/L	0.1 ng/L	(Yang and Westerhoff, 2014)
	sp-ICPMS	Netherlands	0.4–5.2 ng/L	–	(Peters <i>et al.</i> , 2018)

## 2.4 Removal of nanoparticles through conventional water treatment



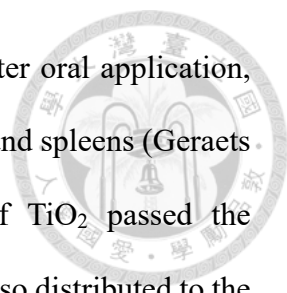
Conventional drinking water treatment typically involves coagulation, sedimentation, filtration and disinfection processes, and is widely applied worldwide. During the coagulation process, coagulants such as polyaluminum chloride (PAC), aluminum sulfate, iron chloride, etc, are added to destabilize the dissolved and suspended particles in the raw water. The destabilized particles aggregate to form larger flocs, which can consequently be removed by gravity sedimentation. Filtration is a process that removes suspended matter and microorganisms by ways of absorption, encapsulation, sedimentation and chemical reactions. The purpose of disinfection is to eliminate or deactivate pathogenic microorganisms, and chlorine is one of the most commonly used disinfectants. With increasing concern to the potential health effects of consuming nanomaterials from drinking water sources, studies have evaluated the removal efficiency through conventional water treatment which helps to better understand the realistic exposure levels of users. Sousa et al. demonstrated that a combination of coagulation, flocculation, and sedimentation (C/F/S) process could effectively remove metal-based engineered nanoparticles through the major mechanism of charge neutralization. The removal efficiency depends on the raw water characteristics, approximately 98% and 99% of Ti can be removed from natural water with low turbidity and medium turbidity, respectively (Sousa and Ribau Teixeira, 2020). Honda et al. concluded that the dominant mechanism of TiO<sub>2</sub> particles removal is sweep flocculation, and by using coagulants such as FeSO<sub>4</sub> and Al<sub>2</sub>(SO<sub>4</sub>)<sub>3</sub>, the removal efficiency could achieve over 90% (Honda *et al.*, 2014). The removal efficiency of TiO<sub>2</sub> particles in artificial groundwater and artificial surface water was reported to be 97.6%±1.7% and 98.7%±1.5%, respectively (Kinsinger



*et al.*, 2015). A study evaluated the breakthrough of nanoparticles during drinking water treatment and found that for TiO<sub>2</sub> nanoparticles, the conventional treatment process resulted in 3% to 8% breakthrough, which means that over 90% of the TiO<sub>2</sub> nanoparticles were removed (Chalew Talia *et al.*, 2013). There were also studies on each stage of primary conventional drinking water treatment. With only treatment of coagulation, removal efficiency of TiO<sub>2</sub> nanoparticles was found to reach 86% in natural lake water (Zhang *et al.*, 2017). Donovan *et al.* indicated that greater than 95% of Ti-containing particles were removed through the process of lime softening followed by alum coagulation (Donovan *et al.*, 2016). In summary, most studies indicate that conventional water treatment can achieve a high removal efficiency of TiO<sub>2</sub> nanoparticles. However, due to the difference in the initial concentration of TiO<sub>2</sub> nanoparticles and the raw water characteristics, the removal efficiency under real-world conditions may differ from that of laboratory experiments.

## 2.5 Toxicity of TiO<sub>2</sub> nanoparticles

Exposure routes and innate characteristics may affect the absorption, distribution, and elimination of nanoparticles, thus can cause diverse health effects on different organ systems. People could be exposed to nanoparticles via inhalation, ingestion, skin contacts and injection. The more likely route of exposure depends on the application of nanoparticles. Due to its application as a food additive and in the production of cosmetics, the general public is more likely to be exposed to engineered nano-TiO<sub>2</sub> through ingestion and skin contact (Warheit and Donner, 2015). Therefore, the possible consequences after oral and dermal exposure to engineered nano-TiO<sub>2</sub> are of great concern. The results of animal experiments show that nano-TiO<sub>2</sub> had limited absorption in the gastrointestinal



tract. Low levels of Ti were detected in mesenteric lymph nodes after oral application, while only a few rat subjects were detected to have Ti in their livers and spleens (Geraets *et al.*, 2014). Approximately 0.6% of the administered dose of TiO<sub>2</sub> passed the gastrointestinal barrier after oral exposure. Nano-TiO<sub>2</sub> particles are also distributed to the liver, lung, kidney, spleen, brain, uterus and skeleton (Kreyling *et al.*, 2017). After oral administration of the nano-TiO<sub>2</sub> suspension, accumulation of TiO<sub>2</sub> was observed in the liver, kidney, spleen, and lung of mice (Wang *et al.*, 2007). Crosera *et al.* pointed out that TiO<sub>2</sub> nanoparticles could only be found in the stratum corneum and epidermis and could not penetrate intact skin (Crosera *et al.*, 2015). Skin penetration studies of TiO<sub>2</sub> particles in sunscreens among minipigs reported that Ti levels in the lymph nodes and liver did not exceed those in the control group (Sadrieh *et al.*, 2010). Meanwhile, although skin samples showed elevated Ti content, TiO<sub>2</sub> nanoparticles did not significantly penetrate through the intact normal epidermis. After entering the systemic circulation, nanoparticles are distributed to tissues through blood, so nanoparticles are commonly accumulated in organs containing reticuloendothelial (RES) tissues with high perfusion, such as liver and spleen. Such results have been observed in several animal experiments investigating nano-TiO<sub>2</sub> exposure (Fabian *et al.*, 2008; Geraets *et al.*, 2014; van Ravenzwaay *et al.*, 2009; Wang *et al.*, 2007). Recent studies investigated the distribution and accumulation of nano-TiO<sub>2</sub> particles in humans. Heringa *et al.* demonstrated the presence of TiO<sub>2</sub> particles in the human liver and spleen, and about 24% of the particles were in the nano-size range (Heringa *et al.*, 2018). Peters *et al.* found TiO<sub>2</sub> particles in the liver, spleen, kidney, jejunum and ileum of dead bodies, with a concentration range of 0.01 to 1.8 mg Ti/kg, and higher concentrations were detected in jejunum and ileum tissues. Most of the Ti in these organs and tissues was in the form of particles, accounting for 80% of the total Ti concentration, and about 17% of them are nanoparticles (Peters *et al.*, 2020). There is

evidence that feces and urine excretion are quite crucial in the elimination of nanoparticles. Animal study of mice showed that the nano-TiO<sub>2</sub> particles were intercepted and excreted through the kidney (Wang *et al.*, 2007). After oral exposure of nano-TiO<sub>2</sub>, most of the administered dose can be detected in the feces of rats (Kreyling *et al.*, 2017).

Although there is no consensus on the toxicological mechanism of various nanoparticles, the oxidative stress is observed in many studies. Past studies have found that exposure to nano-TiO<sub>2</sub> may cause adverse health effects, such as oxidative stress, inflammation, and apoptosis (Becker *et al.*, 2014). After exposing the TiO<sub>2</sub> nanoparticles to the lung tissue, the influx of neutrophils in the lung, protein accumulation in the alveolar lavage fluid, the production of active oxidizing substances in the cells, and the production of proinflammatory mediators can be observed (Moon *et al.*, 2010). Injection experiments have shown that nano-TiO<sub>2</sub> induces inflammation and liver damage through fat accumulation (Silva *et al.*, 2017). Other related physiological effects may also lead to reproductive failure by affecting hormones or hatching enzymes (Muller *et al.*, 2015).

## Chapter 3 Materials and Methods



### 3.1 Water Sample Collection

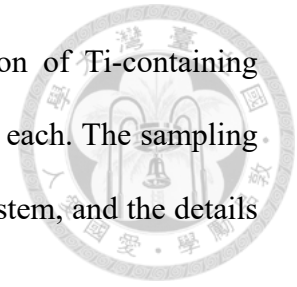
#### 3.1.1 Materials and equipment

1. 100 mL, 1000 mL Teflon PFA bottle (SANPLATEC®, Japan)
2. Nylon rope
3. Aluminum telescopic rod
4. ExStik EC500 a pH, Conductivity, TDS, Salinity and Temperature meter (EXTECH, USA)
5. 2100Q Portable Turbidimeter (HACH, USA)
6. Parafilm (American National Can, Greenwich, CT 06836, USA)
7. 50 mL centrifuge tube (SARSTEDT AG & Co. KG)

#### 3.1.2 Sampling Sites

In this study, we collected samples of raw and finished water from major water treatment plants in the Greater Taipei area, as well as samples from rivers that serve as water sources to the Greater Taipei area. The sampling sites for river water were decided based on the water quality monitoring stations of the EPA and the Taipei Water Specific Area, and the accessibility of the sampling locations was also taken into consideration. In order to reflect the possible exposure of Ti-containing particles to most tap water users in the Greater Taipei area, water treatment plants with higher supply capacity were selected to collect representative samples of raw water and finished water. One conventional water treatment plant was selected from the Keelung River, three plants from the Xindian River, and one plant from the Dahan River were selected, each treatment plant was used to treat

river water. Information on the concentration and size distribution of Ti-containing particles in the raw water and the finished water was obtained from each. The sampling sites were classified according to the tap water intake and supply system, and the details and descriptions are as follows:



1. Keelung River tap water intake and supply system:

The sampling locations of the Keelung River included Sandiaoling in the upper stream, and Ruigan New Village, Jieshou Bridge and Badu Pumping Station in the middle stream. The Badu Pumping Station is the water intake of the Xinshan water treatment plant. Usually, the water from the Badu Pumping Station is directly used, and the excess water is sent to and stored in the Xinshan Reservoir until being supplied to the water treatment plant during the dry season. Xinshan water treatment plant supplies Keelung City and Xizhi District with a designed supply capacity of 200,000 CMD. The current supply capacity for these two regions is about 150,000 m<sup>3</sup>/day.

Table 3-1. Coordinates of sampling sites of the Keelung River tap water intake and supply system.

ID	Sampling site	WGS 84 Coordinates	
		Latitude (N)	Longitude (E)
1-1	Sandiaoling	25.058269	121.821056
1-2	Ruigan New Village	25.106067	121.828496
1-3	Jieshou Bridge	25.106781	121.804525
1-4	Badu Pumping Station	25.111476	121.730097
1-5	Xinshan WTP	25.131388	121.720964

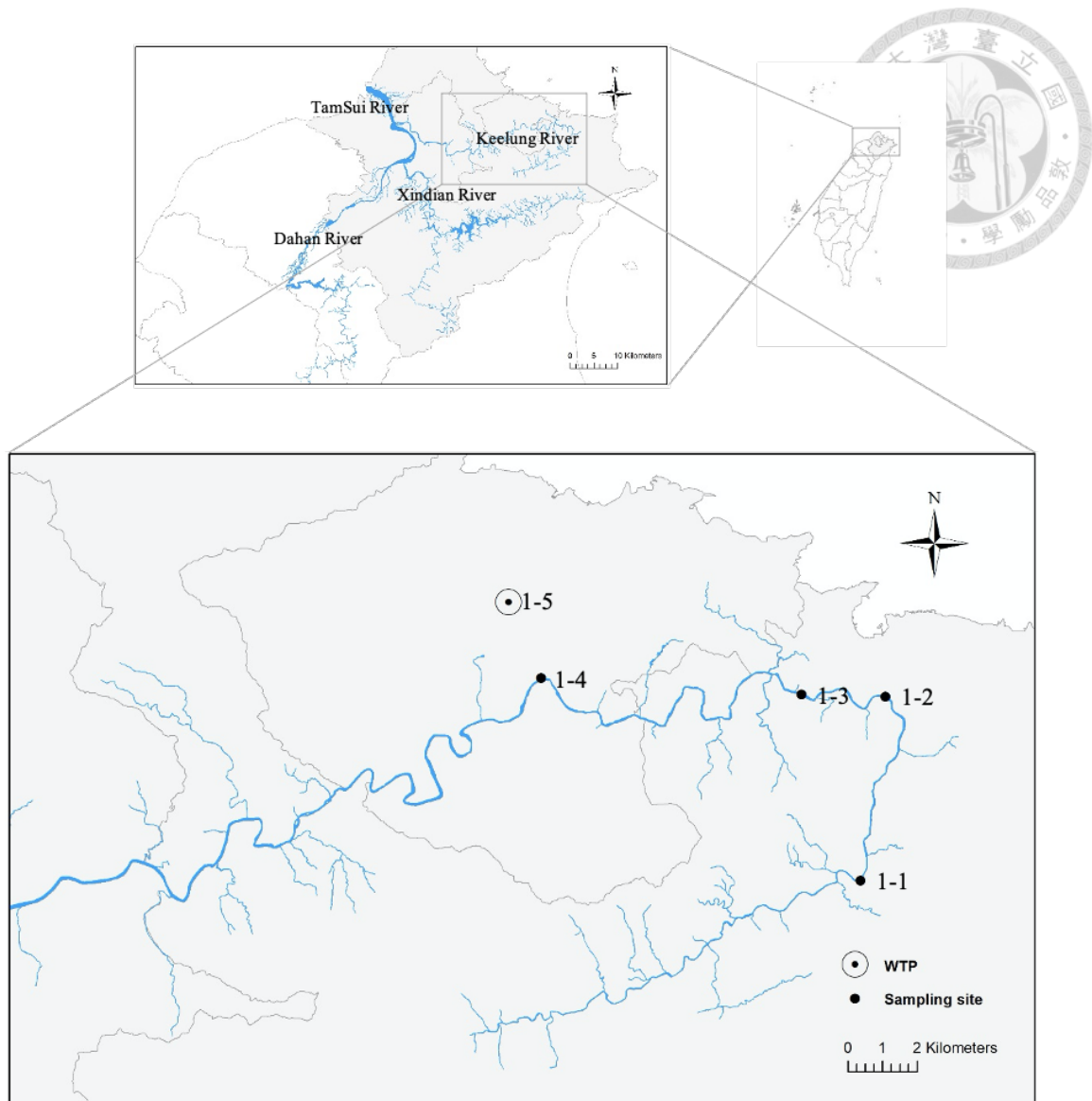


Fig. 3-1 Map of the Keelung River and sampling sites listed in table 3-1.

## 2. Xindian River tap water intake and supply system:

The Xindian River is the primary source of water intake in the Greater Taipei Area, mainly from its upstream the Nanshi River, which is supplemented by the Feitsui Reservoir in the Beishi River as the water intake during shortages from the Nanshi River. The two sampling sites in the Nanshi River were Fushan and Lansheng Bridge, and the two sampling sites in the Beishi River were Kuolai and Dalin Bridge. The sampling sites of the Xindian River included Guangxing Bridge, Zhitan Weir and Qingtan Weir. Zhitan

Weir is the water intake for the Zhitan water treatment plant, and Qingtan Weir is the water intake for the Changxing water treatment plant and the Gongguan water treatment plant. The designed supply capacity of the Zhitan WTP is 1010,000 CMD, including Changxing and Gongguan WTP which are responsible for 97.5% of tap water supply in Taipei City.

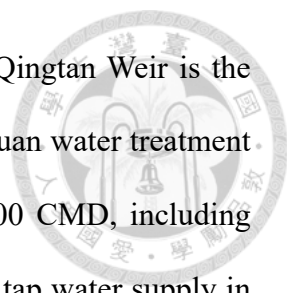


Table 3-2. Coordinates of sampling sites of the Xindian River tap water intake and supply system.

ID	Sampling site	WGS 84 Coordinates	
		Latitude (N)	Longitude (E)
2-1	Fushan	24.780835	121.503406
2-2	Lansheng Bridge	24.862192	121.55137
2-3	Kuolai	24.965009	121.771133
2-4	Dalin Bridge	24.932689	121.705268
2-5	Guangxing Bridge	24.912818	121.547852
2-6	Zhitan Dam	24.926885	121.532315
2-7	Qingtian Dam	24.948103	121.545873
2-8	Zhitan WTP	24.943195	121.527901
2-9	Changxing WTP	25.015276	121.548674
2-10	Gongguan WTP	25.013683	121.531014

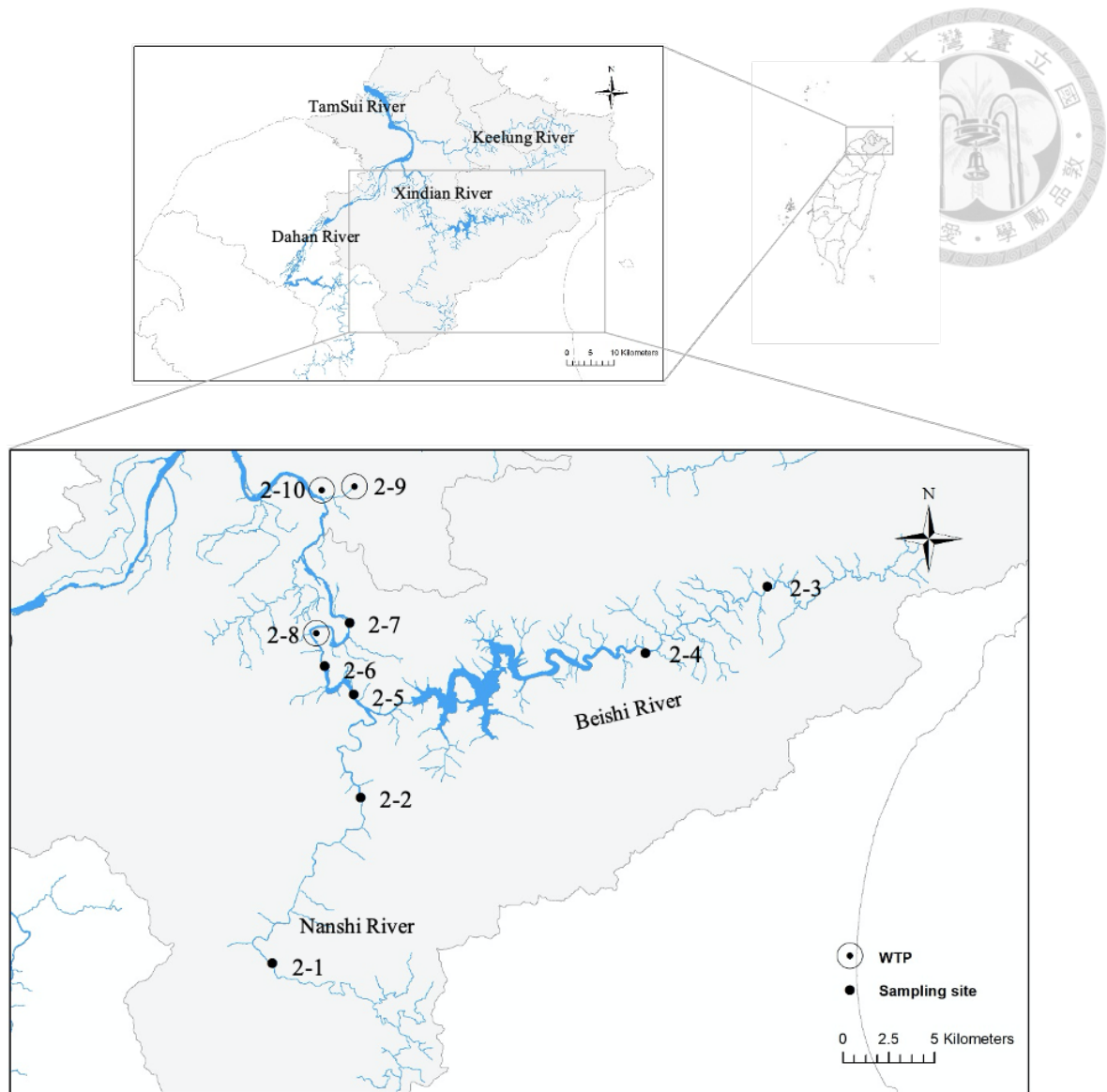


Fig. 3-2 Map of the Xindian River, Beishi River, Nanshi River, and sampling locations listed in table 3-2.

### 3. Dahan River tap water intake and supply system:

The water source for Bansin Water Treatment Plant is mainly from the Dahan River, and is supplemented by the Sanxia River, a tributary of the Dahan River, during water shortages. The sampling sites of the Dahan River include the Afterbay of Shi-Men Reservoir, Daxi Bridge and Yuanshan Weir. The sampling location of the Sanxia River was the Sanxia Pumping Station. The Yuanshan Weir and the Sanxia Pumping Station are

the water intake, from which raw water is delivered to Bansin Water Treatment Plant. Bansin WTP supplies drinking water to the New Taipei City and some Taoyuan areas with daily supply of approximately 680,000 m<sup>3</sup>/day.



Table 3-3. Coordinates of sampling sites of the Dahan River tap water intake and supply system.

ID	Sampling site	WGS 84 Coordinates	
		Latitude (N)	Longitude (E)
3-1	Afterbay	24.822766	121.249764
3-2	Daxi Bridge	24.885326	121.282629
3-3	Yuanshan Weir	24.929194	121.343204
3-4	Bansin WTP	24.940102	121.357139
3-5	Sanxia Pumping Station	24.896042	121.373956

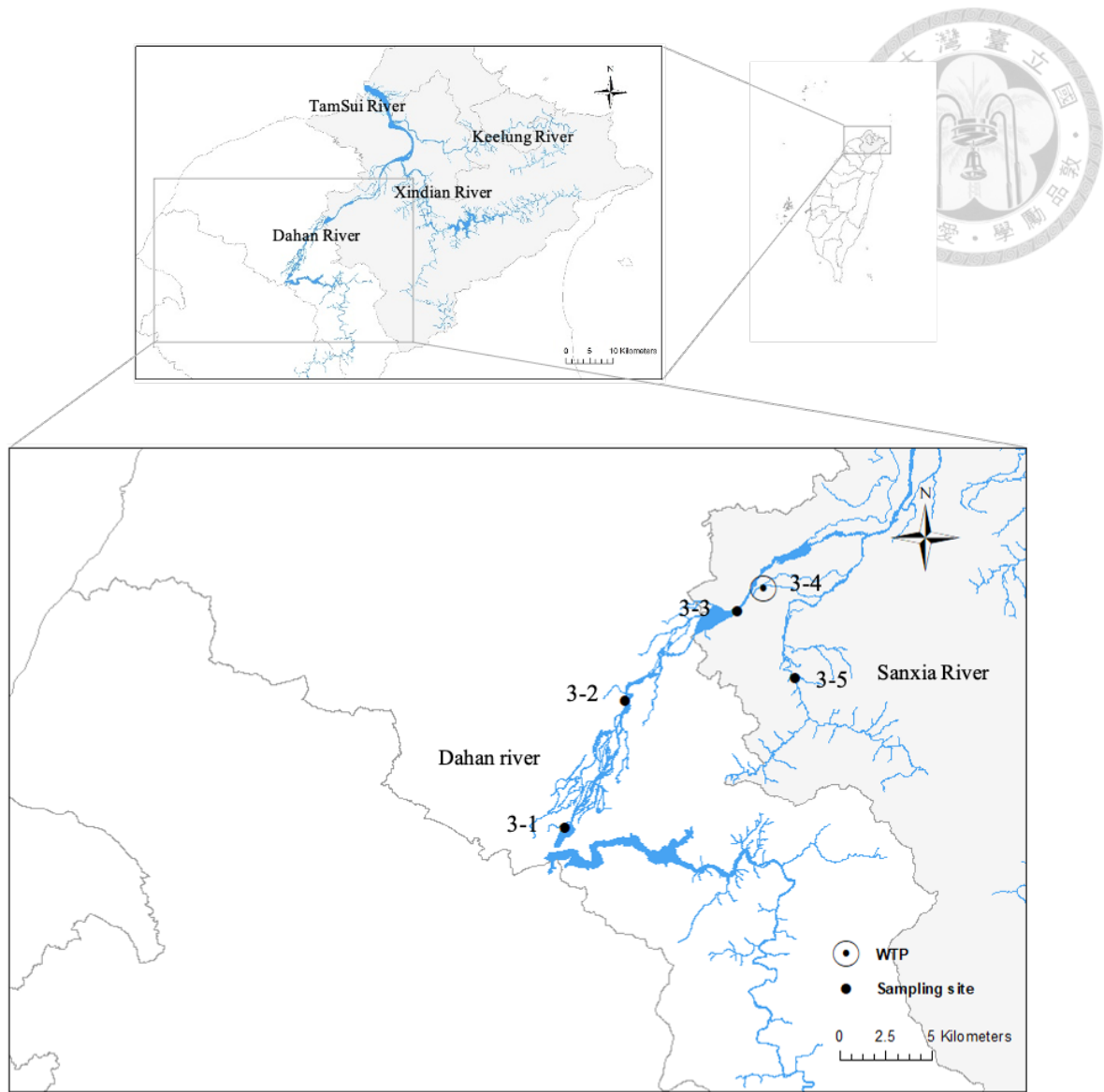


Fig. 3-3 Map of the Dahan River, Sanxia River, and sampling locations listed in table 3-3.

### 3.1.3 Sampling procedure

Considering seasonal river flow variation, samples were collected during the dry period (from February 24 to March 2, 2020) and wet period (from May 25 to June 3, 2020). All samples of the Keelung River and Dahan River tap water intake and supply systems were collected within one day, while the sampling of the Xindian River system was completed within two consecutive days. Rainfall may interfere with the

representativeness of the samples, so, following EPA guidelines for water sampling, sampling in the following situations was avoided: (1) the previous day's rainfall reached 50 mm, (2) seven days after a single-day of rainfall which exceeded 130 mm, or (3) 14 days after a single-day of rainfall which exceeded 200 mm.

Teflon PFA bottles (SANPLATEC®, Japan) were used for sampling, and 50 mL centrifuge tubes (SARSTEDT AG & Co. KG) were used for sample storage. All containers were rinsed several times with double deionized water (DDW) (Millipore, Milli-Q Elix®5/RiOs, USA) and then filled with DDW before used to prevent nanoparticles from being adsorbed on the inner surface of the containers and causing sample contamination.

The methods and tools for river water samples collection depended on the sampling site. Samples were collected from the center of the river by hanging the Teflon PFA bottle with a nylon rope to collect the water samples from the upstream side of the bridge, or by extending the PFA bottle attached to a telescopic rod to collect samples from the riverside. The water sample collected in PFA bottle was then transferred to the 50 mL centrifuge tubes without leaving the headspace. Then the centrifuge tubes filled with water samples were capped with a screw top cap and sealed with parafilm (American National Can, Greenwich, CT 06836, USA).

The raw water and finished water samples were collected from the respective tanks in the water treatment plants. When collecting samples onsite, a Teflon PFA bottle hung on a length of nylon rope was used for sampling. When sampling from the pipeline, for example, in the water quality laboratory, the water samples were directly collected from the tap into the 50 mL centrifuge tubes. Then the centrifuge tubes filled with water samples were capped with a screw top cap and sealed with parafilm.

Transport blanks and field blanks were prepared to confirm whether contamination

occurred during transportation and the sampling process. All collected samples were transported in a cooler back to the laboratory, and stored at 4°C in a dark environment until analysis.



## 3.2 Ti-containing nanoparticles analysis

### 3.2.1 Standards, chemicals, and materials

1. Double deionized water (Millipore, Milli-Q Elix®5/RiOs, USA)
2. Nitric acid (69-70 %, J.T. Baker, USA)
3. Isopropyl alcohol (鴻勝化學科技股份有限公司, Taiwan)
4. 30 nm gold nanospheres (nanoComposix, USA)
5. 100 nm titanium dioxide dispersion (US Research Nanomaterials, Houston)
6. Multi-element calibration standard-4 (Agilent, USA)
7. Gold tuning solution, Au (Agilent, USA)
8. NIST trace elements in water 1643f (NIST, USA)
9. ICP-MS tuning solution (Agilent, USA)
10. 3 mL syringe (Terumo Co. Philippines)
11. 0.45 µm PVDF filter (Recenttec®, Taiwan)
12. 15 mL centrifuge tube (SARSTEDT AG & Co. KG)

### 3.2.2 Sample pretreatment

All samples were diluted with DDW before analysis for TiO<sub>2</sub> nanoparticles. In order to obtain the signal within the optimal range, the dilution ratio was determined based on the preliminary tests. All blank samples and finished water samples were diluted 10 times with DDW. For river water samples and raw water samples collected from the Xindian

River System were diluted 10 times, while those collected from the Keelung River System and Dahan River System were diluted 100 times. An aliquot of 3mL of the diluted sample was filtered using a 0.45  $\mu\text{m}$  PVDF filter (Recenttec®, Taiwan) and stored into a pre-cleaned 15 mL centrifuge tube. Then the centrifuge tubes were placed on the autosampler holder for subsequent analysis.

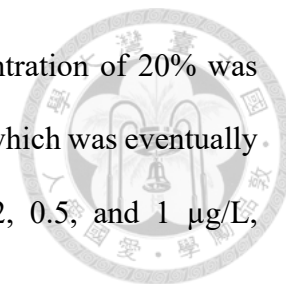
### 3.2.3 Preparation of Calibration Curves

Specific concentrations of ionic and nanoparticle standards for the reference material, i.e., Au in this study, needed to be analyzed with the single particle acquisition mode. The Au tuning solution of 100 mg/L was diluted to 0.1  $\mu\text{g/L}$  and set as the ionic standard for the reference material Ionic Standard (RM), which was used to calculate nebulization efficiency. The 30 nm gold nanospheres suspension of 10 ng/L was set as reference material (RM) to calculate the particle concentration and particle size of the sample. An aliquot of 0.1 mL 30 nm gold nanospheres of 50 mg/L was first mixed with 0.8 mL of pure isopropanol, and then diluted with DDW to make a 50 mL, 100  $\mu\text{g/L}$  stock suspension. The stock suspension was then diluted to the reference concentration of 0.1  $\mu\text{g/L}$ . The purpose of adding the final concentration of 2% isopropanol was to make the nanoparticles evenly dispersed in the solution.

Ionic Ti standard of 1  $\mu\text{g/L}$  was set as the reference concentration of the analyte (Ionic standard, AN), which was  $\text{TiO}_2$  in this study with single particle analysis. Then, an aliquot of 100  $\mu\text{L}$  Multi-element calibration standard-4 solution of 10 mg/L was made up with DDW to prepare a 10 mL, 100  $\mu\text{g/L}$  stock solution, which was in turn diluted to the concentration of 1  $\mu\text{g/L}$ .

The 100 nm  $\text{TiO}_2$  dispersion standard was used for making a calibration curve to calculate the mass concentration and total concentration of  $\text{TiO}_2$  nanoparticles. First, an

aliquot of 0.25 mL standard solution with a weight percent concentration of 20% was diluted with DDW to prepare a 50 mL stock solution of 1000 mg/L, which was eventually diluted to the desired concentration of 0.01, 0.02, 0.05, 0.1, 0.2, 0.5, and 1  $\mu\text{g/L}$ , respectively.



### 3.2.4 Instrumental Analysis

Nano-TiO<sub>2</sub> and total titanium concentration were analyzed using Agilent 8900 Triple Quadrupole ICP-MS. Dwell time was set at 0.1 ms, and data analysis was performed in fast Time Resolved Analysis (TRA) mode. The analysis was operated in mass-shift mode and O<sub>2</sub> mode to eliminate the polyatomic and isobaric interferences on <sup>48</sup>Ti. Detailed operating settings are listed in Table 3-4.

Table 3-4. Single particle acquisition mode operating parameters for sp-ICPMS.

	Parameter	Value
Plasma		
	RF Power	1550 W
	RF Matching	1.40 V
	Sampling Depth	8 mm
	Nebulizer Gas	0.70 L/min
	Nebulizer Pump	0.10 rps
	Spray Chamber Temp.	2°C
	Makeup Gas	0.35 L/min
Lenses		
	Extract 1	0.0 V
	Extract 2	-180.0 V
	Omega Bias	-100.0 V
	Omega Lens	8.0 V

Table 3-4. Single particle acquisition mode operating parameters for sp-ICPMS  
(continued).

Parameter	Value
Q1 Entrance	-5.0 V
Q1 Exit	2.0 V
Cell Focus	-5.0 V
Cell Entrance	-50 V
Cell Exit	-60 V
Deflect	4.0 V
Plate Bias	-50 V

### 3.2.5 Detection Limits

The method detection limit (MDL) for the mass concentration of Ti-containing particles by sp-ICPMS analysis was calculated from equation (1) as follows:

$$MDL_{part.} = \frac{3\sigma}{Slope} \quad (1)$$

where  $\sigma$  is the standard deviation of the particle signal (cps) from the independent analysis of the seven replicate spiked samples with the lowest concentration of the calibration curve. In this study, the  $MDL_{part.}$  for Ti-containing particles was 10.47 ng/L.

Using the equation mentioned by Lee et al., the detection limit ( $LOD_{size}$ ) (Lee et al., 2014) of the particle size of Ti-containing particles was calculated as follows:

$$LOD_{size} = \left( \frac{6 * 3\sigma_{DI}}{R} \right)^{1/3} \quad (2)$$

$$\frac{\eta * \nu * T * f_a * \rho * \pi}{}$$

$\sigma_{DI}$  is the background signals (cps) of DDW;  $R$  is the response factor (cps/ppb) of the analyte;  $\eta$  is the transport efficiency (%);  $\nu$  is the flow rate (mL/min);  $T$  is the dwell time (s);  $f_a$  is the mass fraction of element in the particle; and  $\rho$  is the density of the

particle ( $\text{g}/\text{cm}^3$ ). The  $LOD_{size}$  found in the preliminary test was 2.32 nm (鍾季桓, 2019).



### 3.2.6 QA/QC

Calibration curves were established with at least 5 concentrations for each batch of analysis. The  $R^2$  value of the calibration curve of particle mass concentration and particle number concentration must be  $\geq 0.995$ . Due to the lack of commercially available standard reference materials, a control sample made of 100 nm  $\text{TiO}_2$  suspension with a concentration of 250 ng/L was analyzed in each batch of experiments to verify accuracy. The ratio of the determined value to the reference concentration (250 ng/L) must be between 80% and 120%. To confirm the analysis stability, a spiked sample of 100 ng/L was placed between every ten samples for Ti determination during the analysis. The ratio of the number of particles and the cps value in the spiked samples to the corresponding analysis value of the 100 ng/L standard in the calibration curve must be between 80% and 120%.

## Chapter 4 Results



### 4.1 Distribution of Ti-containing nanoparticles in drinking water sources

#### 4.1.1 Keelung River

##### 1. Total mass concentration

Fig. 4-1-(a) shows the gradually increasing trend in total Ti concentration from upstream to midstream during the dry season. The total concentration ranged from the lowest concentration of  $7.26 \pm 0.39$  ng/mL at Sandiaoling to the highest concentration of  $9.78 \pm 0.53$  ng/mL at the Badu Pumping Station (Table 4-1).

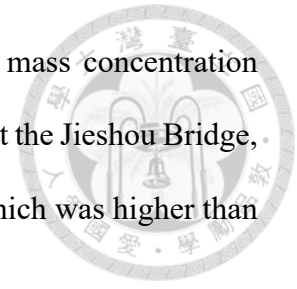
During the wet season, the total concentration gradually increased downstream, from  $6.29 \pm 0.11$  ng/mL at Sandiaoling to  $9.80 \pm 0.35$  ng/mL at the Jieshou Bridge, which was comparable to the concentration range found in the dry season. However, an abrupt increase occurred at the Badu Pumping station and the measured concentration was  $19.4 \pm 0.71$  ng/mL (Table 4-1).

##### 2. Particle mass concentration

The particle mass concentration at each sampling site of the Keelung River was approximately equivalent (Fig. 4-1-(a)). The lowest mass concentration was  $1.14 \pm 0.20$  ng/mL at Ruigan New Village, and the highest was  $1.58 \pm 0.55$  ng/mL at the Badu Pumping Station (Table 4-1).

During the wet season, the particle mass concentration exhibited a similar spatial trend to the total concentration and number concentration, which gradually increased

downstream and rose abruptly at the Badu Pumping Station. The mass concentration ranged from  $2.83 \pm 0.17$  ng/mL at Sandiaoling to  $5.06 \pm 0.25$  ng/mL at the Jieshou Bridge, and increased to  $11.5 \pm 0.45$  ng/mL at the Badu Pumping Station, which was higher than all measured values in the dry season.



### 3. Number concentration

No spatial trend of number concentration was observed during the dry season (Fig. 4-1-(b)). The lowest number concentration was  $170 \pm 20.3 \times 10^3$  part./mL at the Ruigan New Village, and the highest was  $231 \pm 20.3 \times 10^3$  part./mL at Sandiaoling (Table 4-1).

For the wet season, number concentration followed the distribution of total concentration and mass concentration (Fig. 4-1-(e)), and was significantly higher than the concentration levels in the dry season. The number concentration gradually increased downstream from  $1372 \pm 415 \times 10^3$  part./mL at Sandiaoling to  $2029 \pm 532 \times 10^3$  part./mL at the Jieshou Bridge, and the highest concentration of  $4109 \pm 465 \times 10^3$  part./mL was measured at the Badu Pumping Station.

### 4. Most frequent size

We found little seasonal variation in particle size in the Keelung River, and the most frequent sizes of Ti-containing particles among all sampling sites were generally similar, around 40 nm (Fig. 4-1-(c) and (f)). During the dry season, the most frequent size ranged from 36 nm at Sandiaoling and the Jieshou Bridge to 40 nm at Ruigan New Village and Badu Pumping Station. During the wet season, the samples from Ruigan New Village and Badu Pumping Station were found to have a smaller particle size averaging at or around 40 nm, while at the remaining sampling sites the most frequent size ranged from 38 to 42 nm.

The water quality parameters are listed in Table 4-2. Seasonal changes were observed in water temperature, conductivity, TDS, and salinity. The water temperature at each sampling site was higher during the wet season. Conversely, the conductivity, TDS, and salinity values declined in the wet season. Turbidity showed both seasonal and spatial variation. Overall, the turbidity values gradually increased downstream, and were higher during the wet season.

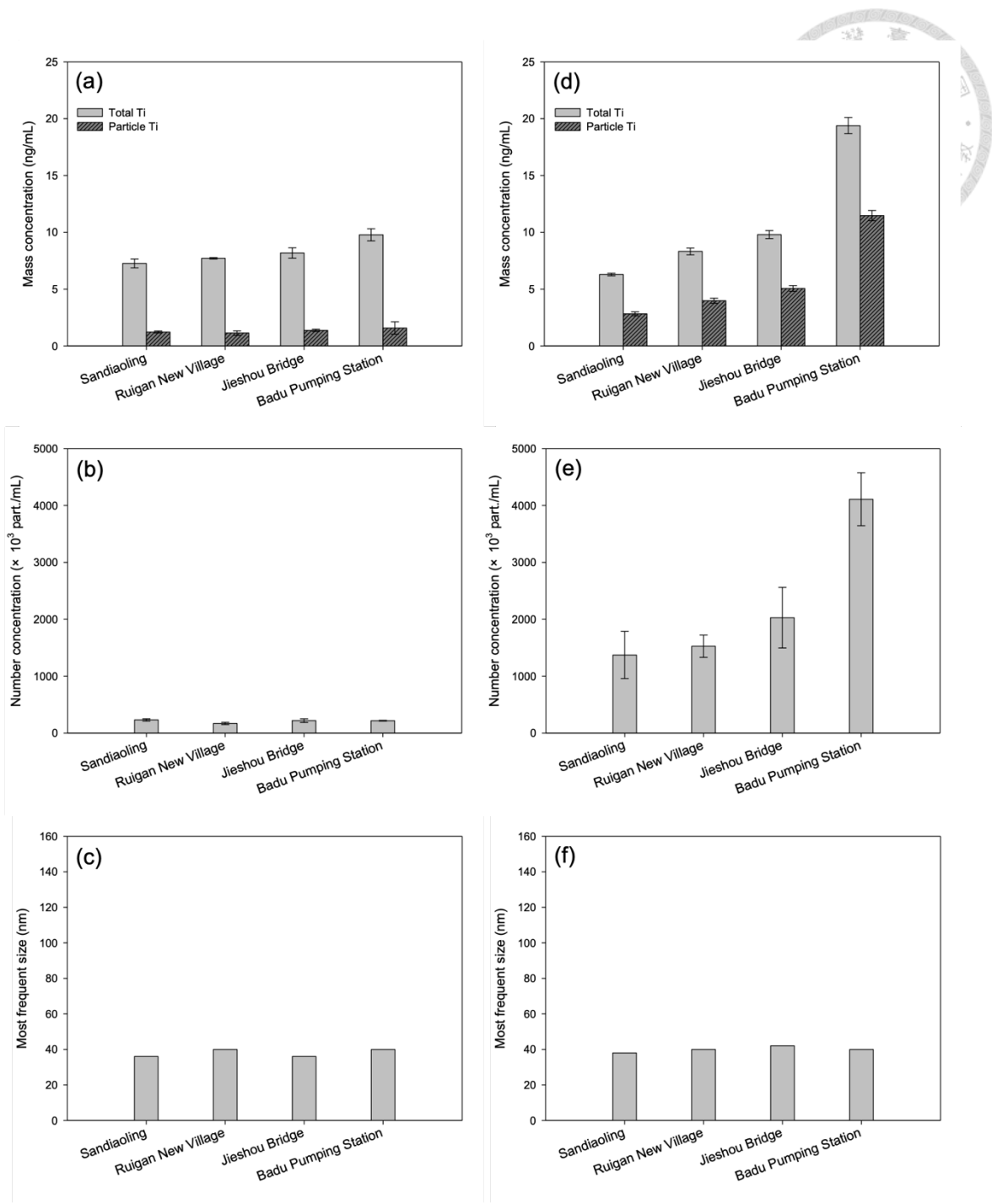


Fig. 4-1 Total Ti and particle Ti mass concentration (a,d), number concentration (b,e), and the most frequent size (c,f) of Ti-containing nanoparticles in the Keelung River.

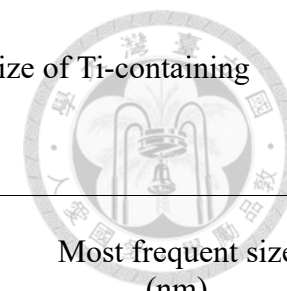
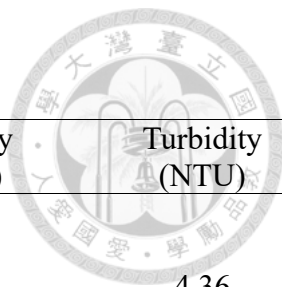


Table 4-1. Total Ti mass concentration, particle Ti mass concentration, number concentration and the most frequent size of Ti-containing nanoparticles in the Keelung River.

	N	Total mass concentration (ng/mL) M ± SD	Particle mass concentration (ng/mL) M ± SD	Number concentration (×10 <sup>3</sup> part./mL) M ± SD	Most frequent size (nm)
<b>Dry season</b>					
Sandiaoling	2	7.26 ± 0.39	1.23 ± 0.09	231 ± 20.3	36
Ruigan New Village	2	7.71 ± 0.06	1.14 ± 0.20	170 ± 20.3	40
Jieshou Bridge	2	8.18 ± 0.46	1.38 ± 0.10	219 ± 31.9	36
Badu Pumping Station	2	9.78 ± 0.53	1.58 ± 0.55	217 ± 5.80	40
<b>Wet season</b>					
Sandiaoling	2	6.29 ± 0.11	2.83 ± 0.17	1372 ± 415	38
Ruigan New Village	2	8.32 ± 0.30	3.98 ± 0.23	1527 ± 196	40
Jieshou Bridge	2	9.80 ± 0.35	5.06 ± 0.25	2029 ± 532	42
Badu Pumping Station	2	19.4 ± 0.71	11.5 ± 0.45	4109 ± 465	40

Table 4-2. Water quality measurements of the Keelung River.



	Temperature (°C)	pH	Conductivity ( $\mu$ S/cm)	TDS (mg/L)	Salinity (ppm)	Turbidity (NTU)
<b>Dry season</b>						
Sandiaoling	18.1	7.95	153.6	138.0	71.5	4.36
Ruigan New Village	17.9	8.18	164.5	148.0	78.0	4.73
Jieshou Bridge	17.5	7.95	172.4	155.0	80.4	4.38
Badu Pumping Station	17.8	7.59	200.0	180.0	95.0	6.67
<b>Wet season</b>						
Sandiaoling	25.4	7.68	93.2	83.6	43.4	11.3
Ruigan New Village	26.7	8.17	106.5	95.2	49.6	15.3
Jieshou Bridge	26.3	7.87	100.0	89.9	47.0	19.9
Badu Pumping Station	27.8	7.58	110.7	99.5	51.7	53.9

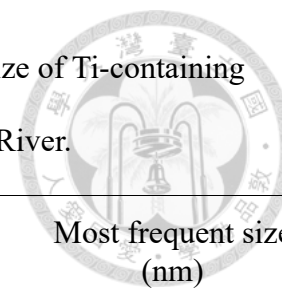


Table 4-3. Total Ti mass concentration, particle Ti mass concentration, number concentration and the most frequent size of Ti-containing nanoparticles in transport blank and field blank samples collected from each sampling site of the Keelung River.

	N	Total mass concentration (ng/mL)	Particle mass concentration (ng/mL)	Number concentration ( $\times 10^3$ part./mL)	Most frequent size (nm)
<b>Dry season</b>					
Transport Blank	1	0.16	0.00	0.00	N.D.
Sandiaoling	1	0.15	0.08	2.46	26
Ruigan New Village	1	0.43	0.08	10.7	34
Jieshou Bridge	1	0.27	0.10	15.2	38
Badu Pumping Station	1	0.28	0.08	0.41	42
<b>Wet season</b>					
Transport Blank	1	0.10	0.10	2.07	30
Sandiaoling	1	0.10	0.09	1.24	28
Ruigan New Village	1	0.10	0.09	16.5	28
Jieshou Bridge	1	0.11	0.09	16.5	28
Badu Pumping Station	1	0.12	0.09	12.4	20



#### 4.1.2 Xindian River and its upstream tributaries

##### 1. Total mass concentration

Overall, the Nanshi River had a relatively high total Ti concentration. The highest measured value was  $7.21 \pm 0.09$  ng/mL at Fushan, followed by  $6.79 \pm 0.01$  ng/mL at Lansheng Bridge during the dry season. The lowest concentration of  $2.19 \pm 0.06$  ng/mL was found at Kuolai, and the total Ti concentration of the Beishi River ranged from  $2.19 \pm 0.06$  ng/mL to  $3.44 \pm 0.04$  ng/mL. The total concentration of the Xindian River was similar to the Beishi River, its main tributary, ranging from  $2.92 \pm 0.00$  ng/mL to  $4.06 \pm 0.16$  ng/mL and showed an increasing trend downstream (Fig.4-2-(d)).

During the wet season, the distribution of the total Ti concentration was generally consistent with that during the dry season. Compared with the values found in the dry season, the total concentration of the Nanshi River decreased to between  $5.10 \pm 0.15$  ng/mL to  $5.64 \pm 0.07$  ng/mL, but remained higher than that of the Beishi River and the Xindian River. The lowest total Ti concentration was also measured at Kuolai, and the concentration range of the Beishi River was  $3.24 \pm 0.07$  ng/mL to  $4.38 \pm 0.03$  ng/mL. The concentration of the Xindian River was  $3.60 \pm 0.09$  ng/mL to  $4.74 \pm 1.45$  ng/mL which was also comparable to that of the Beishi River but no spatial trend was observed.

##### 2. Particle mass concentration

Contrary to the distribution of total concentration, the results from both the dry and wet season showed that higher levels of mass concentration of Ti containing particles was distributed in the Beishi River, followed by the Xindian River and then the Nanshi River. During the dry season, the concentration in the Beishi river was from  $0.08 \pm 0.10$  ng/mL to  $0.31 \pm 0.08$  ng/mL, with the highest concentration discovered at Kuolai. In the Nanshi River, the overall concentration ranged from  $0.05 \pm 0.02$  ng/mL to  $0.12 \pm 0.02$  ng/mL,

with the lowest concentration discovered at Fushan. After confluence, the mass concentration in the Xindian River ranged from  $0.10 \pm 0.05$  ng/mL to  $0.16 \pm 0.04$  ng/mL, and the concentration showed a steady increasing trend downstream.

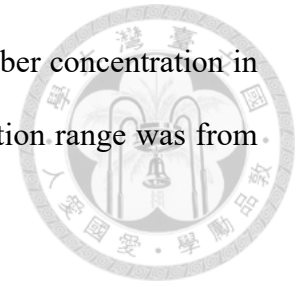
The particle mass concentration levels in the three rivers all showed seasonal change that increased significantly during the wet season. The concentration of the Beishi River, the Nanshi River, and the Xindian River increased from  $1.49 \pm 0.03$  ng/mL to  $1.92 \pm 0.00$  ng/mL,  $0.34 \pm 0.04$  ng/mL to  $0.73 \pm 0.08$  ng/mL, and  $0.53 \pm 0.06$  ng/mL to  $1.67 \pm 1.20$  ng/mL, respectively. However, unlike the spatial trend found in the dry season, the trend that showed increases downstream was observed in both the Beishi River and the Nanshi River, but not in the Xindian River.

### 3. Number concentration

The distribution of the number concentration of Ti containing particles in the three rivers was similar to that of the mass concentration in both dry and wet seasons. During the dry season, the overall number concentration range from high to low in order was  $15.2 \pm 2.72 \times 10^3$  part./mL to  $96.4 \pm 33.9 \times 10^3$  part./mL in the Beishi River,  $14.3 \pm 2.72 \times 10^3$  part./mL to  $42.1 \pm 23.2 \times 10^3$  part./mL in the Xindian River, and then  $5.32 \pm 0.00 \times 10^3$  part./mL to  $5.76 \pm 1.46 \times 10^3$  part./mL in the Nanshi River. The highest concentration of  $96.4 \pm 33.9 \times 10^3$  part./mL and the lowest concentration of  $5.32 \pm 0.00 \times 10^3$  part./mL was found at Kuolai and Fushan, respectively. No consistent spatial trend was observed in each river.

The seasonal variation of the number concentration was similar to that of the mass concentration, showing higher concentration levels during the wet season. Comparable high concentration was  $404 \pm 16.1 \times 10^3$  part./mL to  $417 \pm 26.0 \times 10^3$  part./mL in the Beishi River. In the Nanshi River, number concentration ranged from  $25.6 \pm 3.51 \times 10^3$  part./mL

to  $64.3 \pm 0.88 \times 10^3$  part./mL. There was no spatial trend of the number concentration in the Xindian River during the wet season, and the overall concentration range was from  $111 \pm 9.06 \times 10^3$  part./mL to  $202 \pm 50.6 \times 10^3$  part./mL.



#### 4. Most frequent size

The most frequent sizes of Ti containing particles was found to fluctuate irregularly in all three rivers. During the dry season, the most frequent size ranged from 38 nm to 56 nm, 50 nm to 54 nm, and 44 nm to 56 nm in the Beishi River, the Nanshi River, and the Xindian River. As for the particle size range found in the wet season, it was 44 nm to 46 nm, 50 nm to 66 nm, and 48 nm to 62 nm in the Beishi River, the Nanshi River, and the Xindian River, respectively.

The detailed measurements of water quality are listed in Table 4-5. Compared with the dry season, the water temperature and turbidity values measured at each sampling site increased during the wet season, while the conductivity, TDS, and salinity values were slightly decreased. It was noticed that in Fushan, the conductivity, TDS, and salinity values were all significantly higher than other sampling points during the two sampling periods.

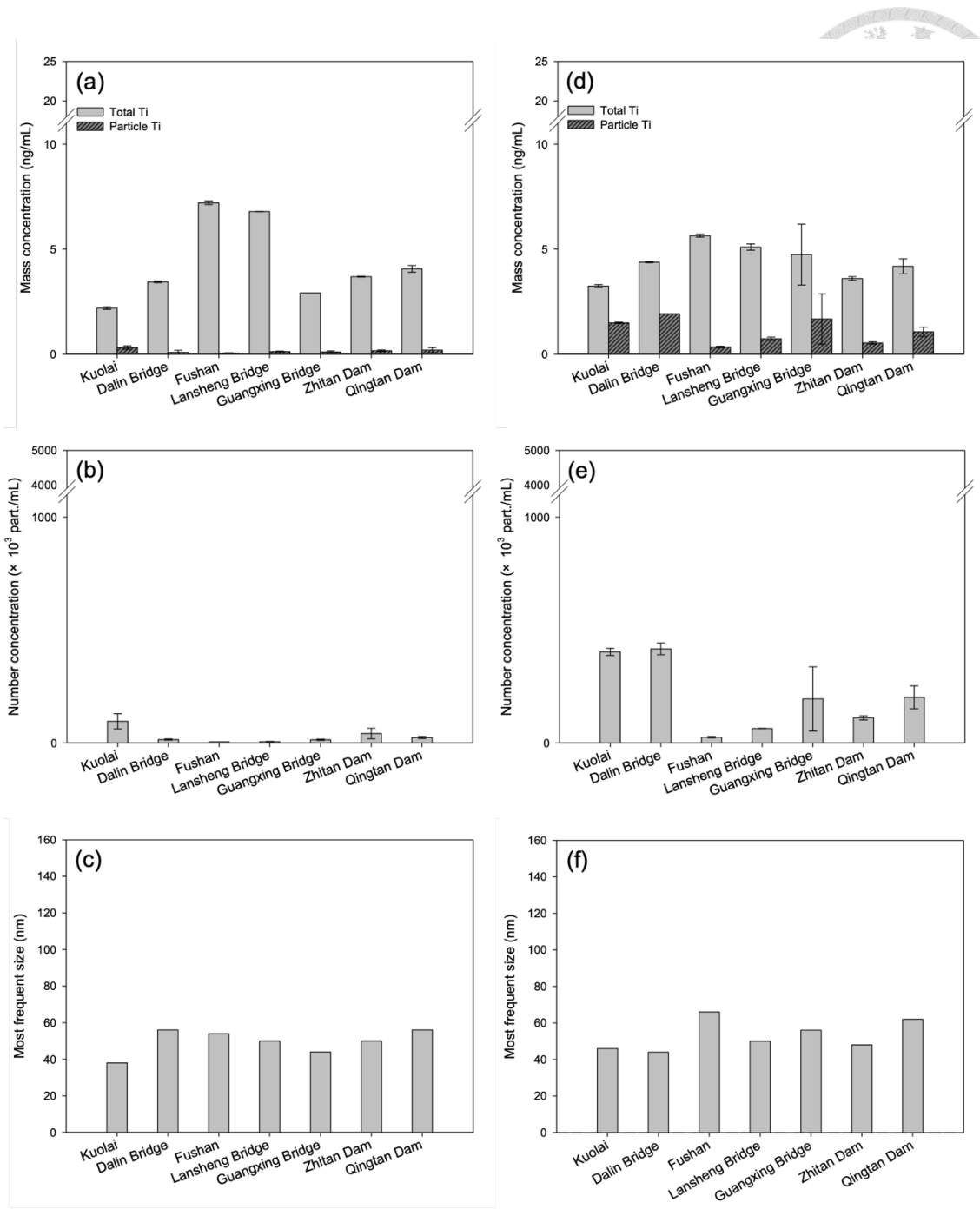


Fig. 4-2 Total Ti and particle Ti mass concentration (a,d), number concentration (b,e), and the most frequent size (c,f) of Ti-containing nanoparticles in the Xindian River and its upstream tributaries.

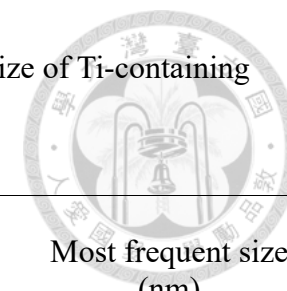


Table 4-4. Total Ti mass concentration, particle Ti mass concentration, number concentration and the most frequent size of Ti-containing nanoparticles in the Xindian River, Beishi River and Nanshi River.

	N	Total mass concentration (ng/mL) M ± SD	Particle mass concentration (ng/mL) M ± SD	Number concentration (×10 <sup>3</sup> part./mL) M ± SD	Most frequent size (nm)
<b>Dry season</b>					
<b>Beishi River</b>					
Kuolai	2	2.19 ± 0.06	0.31 ± 0.08	96.4 ± 33.9	38
Dalin Bridge	2	3.44 ± 0.04	0.08 ± 0.10	15.2 ± 2.72	56
<b>Nanshi River</b>					
Fushan	2	7.21 ± 0.09	0.05 ± 0.02	5.32 ± 0.00	54
Lansheng Bridge	2	6.79 ± 0.01	0.12 ± 0.02	5.76 ± 1.46	50
<b>Xindian River</b>					
Guangxing Bridge	2	2.92 ± 0.00	0.10 ± 0.05	14.3 ± 2.72	44
Zhitan Dam	2	3.69 ± 0.02	0.16 ± 0.04	42.1 ± 23.2	50
Qingtian Dam	2	4.06 ± 0.16	0.19 ± 0.12	24.4 ± 4.81	56

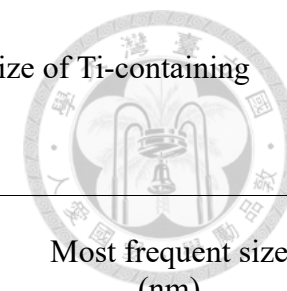


Table 4-4. Total Ti mass concentration, particle Ti mass concentration, number concentration and the most frequent size of Ti-containing nanoparticles in the Xindian River, Beishi River and Nanshi River (continued).

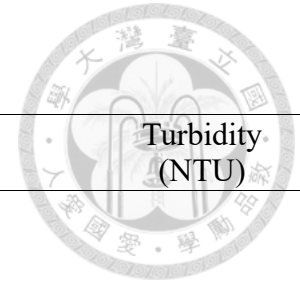
	N	Total mass concentration (ng/mL) M ± SD	Particle mass concentration (ng/mL) M ± SD	Number concentration (×10 <sup>3</sup> part./mL) M ± SD	Most frequent size (nm)
<b>Wet season</b>					
<b>Beishi River</b>					
Kuolai	2	3.24 ± 0.07	1.49 ± 0.03	403 ± 16.1	46
Dalin Bridge	2	4.38 ± 0.03	1.92 ± 0.00	417 ± 26.0	44
<b>Nanshi River</b>					
Fushan	2	5.64 ± 0.07	0.34 ± 0.04	25.6 ± 3.51	66
Lansheng Bridge	2	5.10 ± 0.15	0.73 ± 0.08	64.3 ± 0.88	50
<b>Xindian River</b>					
Guangxing Bridge	2	4.74 ± 1.45	1.67 ± 1.20	195 ± 143	56
Zhitán Dam	2	3.60 ± 0.09	0.53 ± 0.06	111 ± 9.06	48
Qingtán Dam	2	4.18 ± 0.36	1.06 ± 0.22	202 ± 50.6	62



Table 4-5. Water quality measurements of the Xindian River and its tributaries.

	Temperature (°C)	pH	Conductivity ( $\mu$ S/cm)	TDS (mg/L)	Salinity (ppm)	Turbidity (NTU)
<b>Dry season</b>						
<b>Beishi River</b>						
Kuolai	19.1	7.99	63.8	57.4	30.2	1.45
Dalin Bridge	20.8	8.33	89.3	80.4	41.5	1.58
<b>Nanshi River</b>						
Fushan	18.5	8.31	130.6	117.5	61.3	0.63
Lansheng Bridge	19.6	8.04	126.9	114.2	59.0	1.59
<b>Xindian River</b>						
Guangxing Bridge	20.5	7.38	76.7	69.0	34.3	2.31
Zhitán Dam	17.9	7.63	97.7	87.9	44.8	1.84
Qingtán Dam	20.7	7.71	104.2	93.8	49.3	2.89

Table 4-5. Water quality measurements of the Xindian River and its tributaries (continued).



	Temperature (°C)	pH	Conductivity ( $\mu$ S/cm)	TDS (mg/L)	Salinity (ppm)	Turbidity (NTU)
<b>Wet season</b>						
<b>Beishi River</b>						
Kuolai	24.6	7.32	53.5	47.9	24.8	2.08
Dalin Bridge	24.5	7.66	65.7	59.0	30.8	6.08
<b>Nanshi River</b>						
Fushan	23.9	7.98	109.9	98.8	51.5	3.39
Lansheng Bridge	24.1	7.81	94.6	84.9	44.0	5.81
<b>Xindian River</b>						
Guangxing Bridge	23.2	7.25	77.0	69.2	35.8	16.0
Zhitán Dam	25.0	7.52	87.8	77.2	39.4	4.90
Qingtán Dam	24.6	7.49	81.6	72.9	37.5	7.47

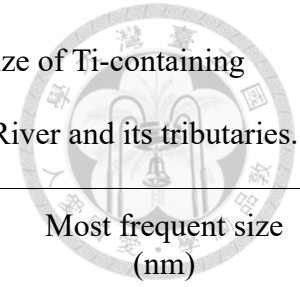


Table 4-6. Total Ti mass concentration, particle Ti mass concentration, number concentration and the most frequent size of Ti-containing nanoparticles in transport blank and field blank samples collected from each sampling site of the Xindian River and its tributaries.

	N	Total mass concentration (ng/mL)	Particle mass concentration (ng/mL)	Number concentration ( $\times 10^3$ part./mL)	Most frequent size (nm)
<b>Dry season</b>					
Transport Blank	1	0.22	0.06	2.36	34
<b>Beishi River</b>					
Kuolai	1	0.18	0.01	0.30	38
Dalin Bridge	1	0.19	0.16	1.77	60
<b>Nanshi River</b>					
Fushan	1	0.16	0.01	2.07	38
Lansheng Bridge	1	0.40	0.15	3.84	32
<b>Xindian River</b>					
Guangxing Bridge	1	0.17	0.10	9.16	32
Transport Blank	1	0.14	0.01	0.89	32
Zhitian Dam	1	0.16	0.01	7.09	42
Qingtian Dam	1	0.03	0.01	2.66	42

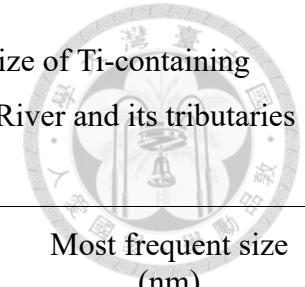


Table 4-6. Total Ti mass concentration, particle Ti mass concentration, number concentration and the most frequent size of Ti-containing nanoparticles in transport blank and field blank samples collected from each sampling site of the Xindian River and its tributaries (continued).

	N	Total mass concentration (ng/mL)	Particle mass concentration (ng/mL)	Number concentration ( $\times 10^3$ part./mL)	Most frequent size (nm)
<b>Wet season</b>					
Transport Blank	1	0.16	0.10	1.65	52
<b>Beishi River</b>					
Kuolai	1	0.07	0.09	1.24	30
Dalin Bridge	1	0.10	0.10	1.65	66
<b>Nanshi River</b>					
Fushan	1	0.07	0.10	1.24	36
Lansheng Bridge	1	0.11	0.14	2.07	62
<b>Xindian River</b>					
Guangxing Bridge	1	0.07	0.10	1.24	30
Transport Blank	1	0.11	0.09	1.24	30
Zhitán Dam	1	0.09	0.09	2.07	34
Qingtán Dam	1	0.13	0.10	0.83	68



### 4.1.3 Dahan River and its tributary

#### 1. Total mass concentration

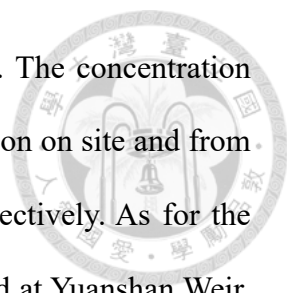
During the dry season, the total Ti concentration in the Dahan River did not show much spatial variation (Fig. 4-3-(a)), and the concentration range was from  $14.0 \pm 0.11$  ng/mL at After Bay to  $15.9 \pm 1.35$  ng/mL at Daxi Bridge. The lowest concentration value of  $10.6 \pm 0.15$  ng/mL was found in samples from the Sanxia River, a tributary of the Dahan River (Table 4-7).

The total Ti concentrations measured at all sampling sites were higher during the wet season (Fig. 4-3-(a) and (d)). The concentration range in the Dahan River ranged from  $15.4 \pm 0.08$  ng/mL at After Bay to  $21.2 \pm 0.19$  ng/mL at Yuanshan Weir, showed a spatial trend of increasing downstream (Fig.4-3-(d)). Noticeable seasonal variations in the total Ti concentration were also observed in the Sanxia River. The samples of the Sanxia River Pumping Station were collected on site and from the reservoir at the Bansin WTP. The measured values were  $17.6 \pm 0.20$  ng/mL and  $22.5 \pm 1.50$  ng/mL respectively, which were higher than those found in the dry season (Table 4-7).

#### 2. Particle mass concentration

In the dry season, except for the higher particle mass concentration of  $1.64 \pm 0.07$  ng/mL observed at Yuanshan Weir, the particle mass concentrations at other sampling sites of Dahan River were similar, ranging from  $0.80 \pm 0.03$  ng/mL to  $0.83 \pm 0.23$  ng/mL. Comparatively low concentrations were found to be  $0.72 \pm 0.04$  ng/mL in the samples of the Sanxia River (Table 4-7).

Compared with the dry season, the particle mass concentration levels of the Dahan River and the Sanxia River increased significantly in the wet season (Fig. 4-3-(a) and (d)). Relatively higher concentrations were found in the Sanxia River instead of the Dahan



River, which differed from our observations during the dry season. The concentration values of the samples collected from the Sanxia River Pumping Station on site and from the reservoir were  $11.3 \pm 0.43$  ng/mL and  $12.2 \pm 1.03$  ng/mL respectively. As for the Dahan River, a higher concentration of  $9.94 \pm 0.26$  ng/mL was found at Yuanshan Weir, and the rest of the measured values were similar, ranging from  $5.49 \pm 0.62$  ng/mL to  $5.65 \pm 0.05$  ng/mL (Table 4-7).

### 3. Number concentration

The number concentration in the Dahan River showed a trend of increasing downstream in both the dry and wet seasons (Fig. 4-3-(b) and (e)). The number concentration range was  $133 \pm 29.3 \times 10^3$  part./mL at After Bay to  $221 \pm 1.46 \times 10^3$  part./mL at Yuanshan Weir in dry season. During the wet season, the number concentration increased significantly and showed a greater spatial variation in concentration compared to that in dry season, ranging from  $666 \pm 85.0 \times 10^3$  part./mL at After Bay to  $2591 \pm 655 \times 10^3$  part./mL at Yuanshan Weir.

The number concentration of the Sanxia River showed the similar seasonal variation trend, which increased significantly in the wet season (Fig.4-3-(e)). The highest concentration was found to be  $4162 \pm 63.0 \times 10^3$  part./mL in the samples collected from the reservoir during the wet season, while the concentration levels in the remaining samples were comparable to those in the Dahan River (Table 4-7).

### 4. Most frequent size

The most frequent size of Ti containing particles in both the Dahan River and Sanxia River showed a consistent seasonal variation trend, that the most frequent size measured at each sampling site became smaller during the wet season (Fig. 4-3-(c) and (f)). The

most frequent size range in the Dahan River was 52 nm to 76 nm in the dry season and 38 nm to 52 nm in the wet season. The most frequent size in the Sanxia River was smaller than that in the Dahan River, 52 nm in the dry season, and 46 nm and 42 nm in the wet season (Table 4-7).

The detailed measurements of water quality are listed in Table 4-8. Compared with the dry season, the water temperature increased while the pH value showed a slight decrease at all sampling sites during the wet season. There was no consistent seasonal trend in conductivity, TDS, salinity and turbidity. Significant decrease in turbidity was observed at the Daxi Bridge during the wet season. The highest turbidity values were measured at After Bay in both the dry and wet seasons.

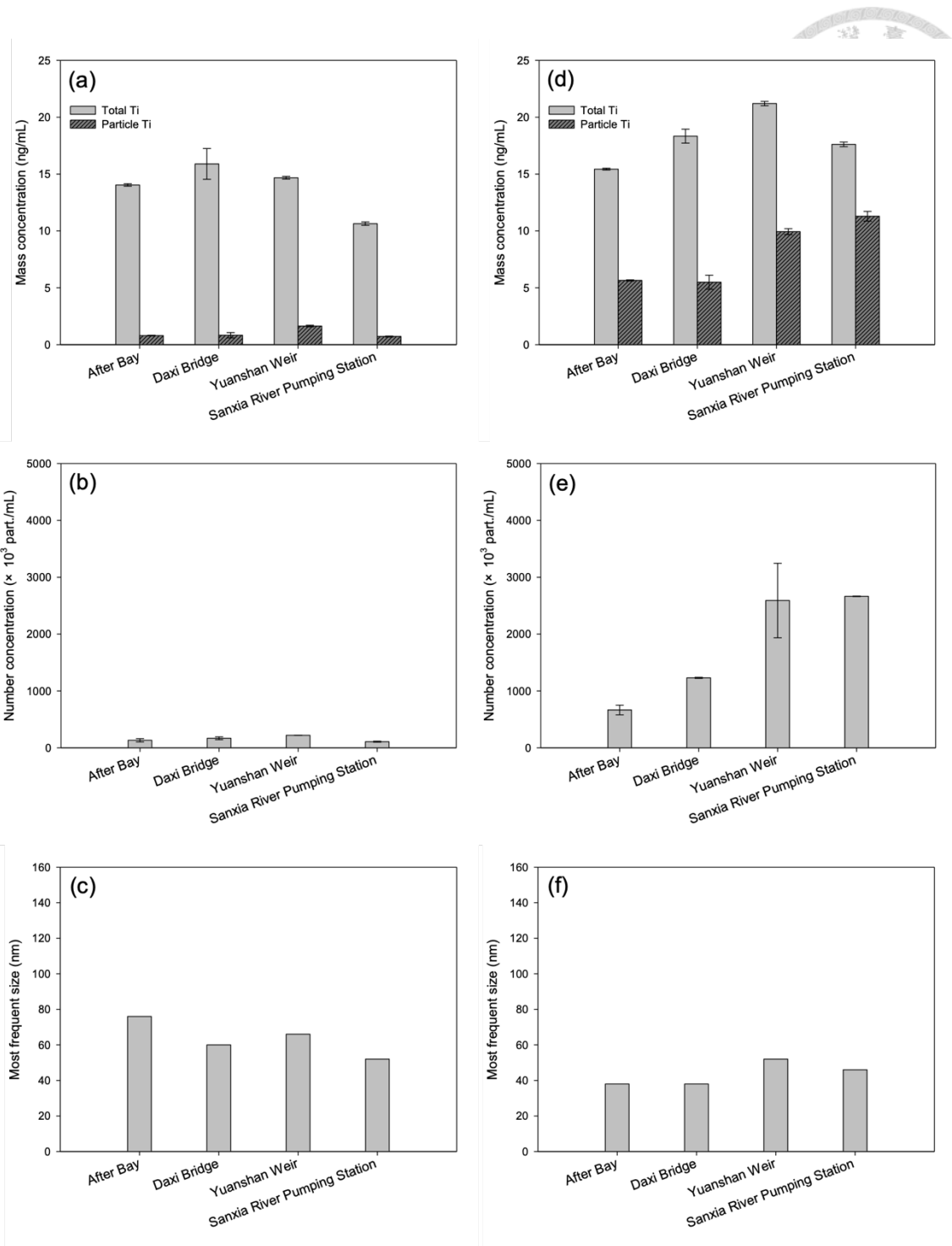


Fig. 4-3 Total Ti and particle Ti mass concentration (a,d), number concentration (b,e), and the most frequent size (c,f) of Ti-containing nanoparticles in the Dahan River and its tributary.

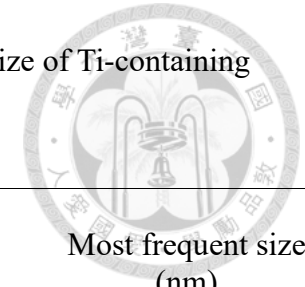


Table 4-7. Total Ti mass concentration, particle Ti mass concentration, number concentration and the most frequent size of Ti-containing nanoparticles in the Dahan River and its tributary.

	N	Total mass concentration (ng/mL) M ± SD	Particle mass concentration (ng/mL) M ± SD	Number concentration (×10 <sup>3</sup> part./mL) M ± SD	Most frequent size (nm)
<b>Dry season</b>					
<b>Dahan River</b>					
After Bay	2	14.0 ± 0.11	0.80 ± 0.03	133 ± 29.3	76
Daxi Bridge	2	15.9 ± 1.35	0.83 ± 0.23	168 ± 25.1	60
Yuanshan Weir	2	14.7 ± 0.12	1.64 ± 0.07	221 ± 1.46	66
<b>Sanxia River</b>					
Sanxia River Pumping Station <sup>b</sup>	2	10.6 ± 0.15	0.72 ± 0.04	108 ± 8.36	52
<b>Wet season</b>					
<b>Dahan River</b>					
After Bay	2	15.4 ± 0.08	5.65 ± 0.05	666 ± 85.0	38
Daxi Bridge	2	18.3 ± 0.61	5.49 ± 0.62	1231 ± 9.44	38
Yuanshan Weir	2	21.2 ± 0.19	9.94 ± 0.26	2591 ± 655	52

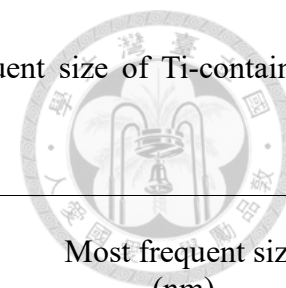


Table 4-7. Total Ti mass concentration, particle Ti mass concentration, number concentration and the most frequent size of Ti-containing nanoparticles in the Dahan River and its tributary (continued).

	N	Total mass concentration (ng/mL) M ± SD	Particle mass concentration (ng/mL) M ± SD	Number concentration (×10 <sup>3</sup> part./mL) M ± SD	Most frequent size (nm)
<b>Wet season</b>					
<b>Sanxia River</b>					
Sanxia River Pumping Station <sup>a</sup>	2	17.6 ± 0.20	11.3 ± 0.43	2664 ± 3.15	46
Sanxia River Pumping Station <sup>b</sup>	2	22.5 ± 1.50	12.2 ± 1.03	4162 ± 63.0	42

<sup>a</sup> Samples collected onsite at the Sanxia River Pumping Station.

<sup>b</sup> Samples collected from the reservoir in the Bansin WTP.

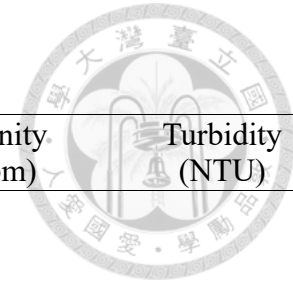


Table 4-8. Water quality measurements of the Dahan River.

	Temperature (°C)	pH	Conductivity (μS/cm)	TDS (mg/L)	Salinity (ppm)	Turbidity (NTU)
<b>Dry season</b>						
<b>Dahan River</b>						
After Bay	19.6	8.13	201.0	180.9	96.0	115
Daxi Bridge	23.7	8.22	221.0	197.0	103.9	85.4
Yuanshan Weir	25.6	9.52	237.0	213.3	112.0	13.8
<b>Sanxia River</b>						
Sanxia River Pumping Station <sup>b</sup>	21.5	8.63	191.0	173.0	89.8	7.72
<b>Wet season</b>						
<b>Dahan River</b>						
After Bay	26.0	7.92	240.0	217.0	113.0	105
Daxi Bridge	27.9	7.74	281.0	250.0	133.0	20.7
Yuanshan Weir	27.7	9.32	201.0	180.0	94.0	33.8
<b>Sanxia River</b>						
Sanxia River Pumping Station <sup>a</sup>	25.0	7.93	138.2	124.6	63.0	23.6
Sanxia River Pumping Station <sup>b</sup>	27.8	7.82	174.9	157.6	82.9	23.6

<sup>a</sup> Samples collected onsite at the Sanxia River Pumping Station. <sup>b</sup> Samples collected from the reservoir in the Bansin WTP.

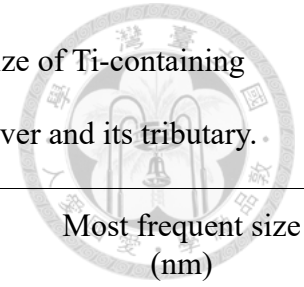


Table 4-9. Total Ti mass concentration, particle Ti mass concentration, number concentration and the most frequent size of Ti-containing nanoparticles in transport blank and field blank samples collected from each sampling site of the Dahan River and its tributary.

	N	Total mass concentration (ng/mL)	Particle mass concentration (ng/mL)	Number concentration ( $\times 10^3$ part./mL)	Most frequent size (nm)
<b>Dry season</b>					
<b>Dahan River</b>					
Transport Blank	1	0.17	0.01	1.48	36
After Bay	1	0.17	0.01	2.36	38
Daxi Bridge	1	0.25	0.01	5.91	32
Yuanshan Weir	1	0.18	0.01	1.77	40
<b>Wet season</b>					
<b>Dahan River</b>					
Transport Blank	1	0.30	0.26	1.34	32
After Bay	1	0.35	0.30	1.34	34
Daxi Bridge	1	0.32	0.26	0.89	26
Yuanshan Weir	1	0.35	0.26	0.45	30
<b>Sanxia River</b>					
Sanxia River Pumping Station	1	0.31	0.26	0.89	26

## 4.2 Distribution of Ti-containing nanoparticles in drinking water systems



### 4.2.1 Drinking water from the Keelung River

#### 1. Total mass concentration

The total Ti concentration in the raw water during the dry season was  $10.2 \pm 0.85$  ng/mL, and decreased to  $7.00 \pm 0.07$  ng/mL after all water treatment processes. As for the wet season, the total concentrations of raw water and finished water during the wet season were  $17.4 \pm 0.87$  ng/mL and  $3.40 \pm 0.07$  ng/mL, respectively, showing a larger decline after treatment compared to the dry season (Fig. 4-4-(a) and (d)).

#### 2. Particle mass concentration

During the dry season, the mass concentration of Ti-containing particles in raw water was  $1.45 \pm 0.13$  ng/mL, and decreased to  $0.09 \pm 0.00$  ng/mL in the finished water, indicating that approximately 94% of the Ti-containing particles were removed through water treatment. An increase in removal efficiency was observed during the wet season (Fig. 4-4-(a) and (d)). The mass concentrations in raw water and finished water were  $10.1 \pm 0.64$  ng/mL and  $0.14 \pm 0.06$  ng/mL, respectively, and the removal rate for Ti-containing particles was about 99% (Table 4-10).

#### 3. Number concentration

The number concentration of Ti-containing particles was  $424 \pm 14.5 \times 10^3$  part./mL in raw water, and decreased to  $7.59 \pm 0.29 \times 10^3$  part./mL in finished water during the dry season. Similar to the seasonal variation trend of mass concentration, the number concentration of Ti-containing particles in raw water increased during the wet season,

reaching a concentration of  $3262 \pm 172 \times 10^3$  part./mL, and decreased to  $105 \pm 0.29 \times 10^3$  part./mL in finished water after water treatment process (Table 4-10).



#### 4. Most frequent size

During the dry season, the most frequent size of Ti-containing particles in raw water was 32 nm, and increased to 48 nm in finished water after the water treatment processes. A similar trend was also observed during the wet season (Fig. 4-4-(f)). The most frequent size of Ti-containing particles in raw water was 42 nm, and a larger particle size of 44 nm was measured in finished water (Table 4-10).

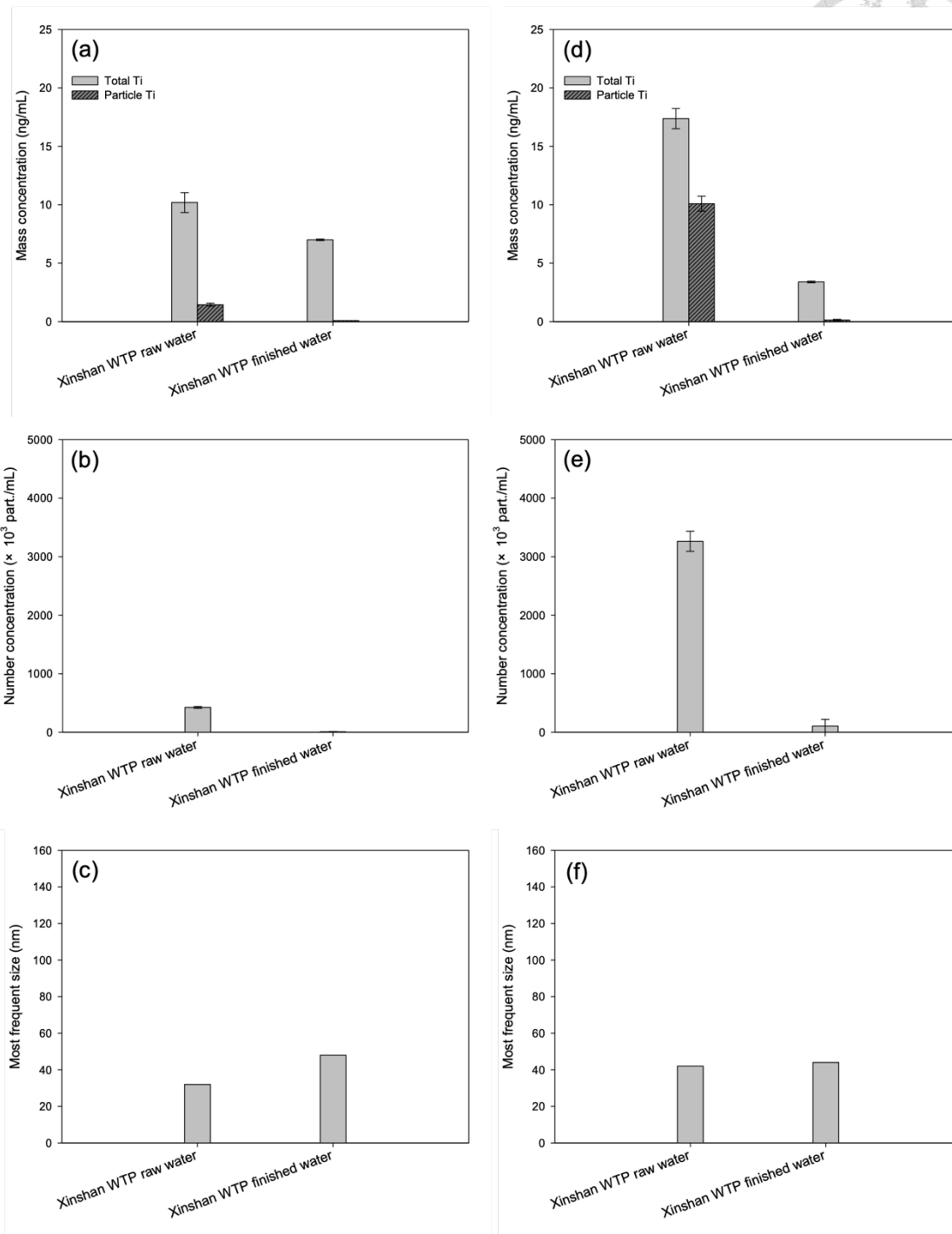


Fig. 4-4 Total Ti and particle Ti mass concentration (a,d), number concentration (b,e), and the most frequent size (c,f) of Ti-containing nanoparticles in raw water and finished water from the Xinshan WTP.

## 4.2.2 Drinking water from the Xindian River

### 1. Total mass concentration

The total Ti concentration of raw water was  $3.44 \pm 0.01$  ng/mL to  $3.79 \pm 0.11$  ng/mL in the dry season and  $3.61 \pm 0.06$  ng/mL to  $4.25 \pm 0.16$  ng/mL in the wet season (Fig. 4-5-(a) and (d)).

Inconsistent changes in the total Ti concentration after water treatment were observed. In the dry season, the concentration of Ti found in finished water in the Zhitan WTP was  $3.43 \pm 0.00$  ng/mL, which was equivalent to the concentration found in raw water. However, the concentration of finished water at the Changxing WTP and Gongguan WTP were  $3.94 \pm 0.16$  ng/mL and  $3.86 \pm 0.01$  ng/mL respectively, both of which were slightly higher than the concentration in raw water. As for the wet season, the total Ti concentration of finished water ranged from  $2.87 \pm 0.00$  ng/mL to  $2.96 \pm 0.02$  ng/mL, showing that the total concentration decreased after passing through the treatment processes.

### 2. Particle mass concentration

In the dry season, the particle mass concentration of Ti containing particles ranged from  $0.13 \pm 0.02$  ng/mL to  $0.24 \pm 0.05$  ng/mL in raw water and decreased to  $0.01 \pm 0.00$  ng/mL to  $0.01 \pm 0.01$  ng/mL in finished water, suggesting that about 92% to 96% of Ti containing particles were removed through the water treatment process.

The particle mass concentration of the raw water rose to  $0.60 \pm 0.05$  ng/mL to  $1.16 \pm 0.12$  ng/mL during the wet season, and the concentration dropped to  $0.09 \pm 0.00$  ng/mL to  $0.10 \pm 0.00$  ng/mL in finished water. The removal rate of Ti containing particles was 88% and 99%, lower than the efficiency observed in the dry season.





### 3. Number concentration

The number concentration of Ti containing particles in raw water ranged from  $42.1 \pm 32.0 \times 10^3$  part./mL to  $72.1 \pm 5.43 \times 10^3$  part./mL and from  $104 \pm 52.6 \times 10^3$  part./mL to  $206 \pm 31.6 \times 10^3$  part./mL in the dry and wet seasons, respectively. As for the finished water, the concentration was  $1.03 \pm 0.21 \times 10^3$  part./mL to  $3.54 \pm 2.10 \times 10^3$  part./mL in the dry season and  $0.41 \pm 0.00 \times 10^3$  part./mL to  $3.94 \pm 4.38 \times 10^3$  part./mL in the wet season, both of which were lower than the values found in raw water.

### 4. Most frequent size

As can be seen in Fig. 4-5-(c) and (f), the alteration in particle size of Ti containing particles after water treatment was irregular. During the dry season, the most frequent size measured increased from 48 nm to 54 nm in the samples from the Zhitan WTP. Conversely, the most frequent size measured decreased from 54 nm to 48 nm in the samples from the Changxing WTP. The most frequent size of the finished water samples from the Gongguan WTP was relatively larger, measuring up to 58 nm.

Contrary to our observations in the dry season, the most frequent size of Ti containing particles in raw water and finished water from the Zhitan WTP were 44 nm and 42 nm, respectively, showing that particle size decreased after treatment processes. The most frequent size measured in finished water from the Changxing and Gongguan WTP both decreased, from 66 nm to 44 nm and 46 nm.

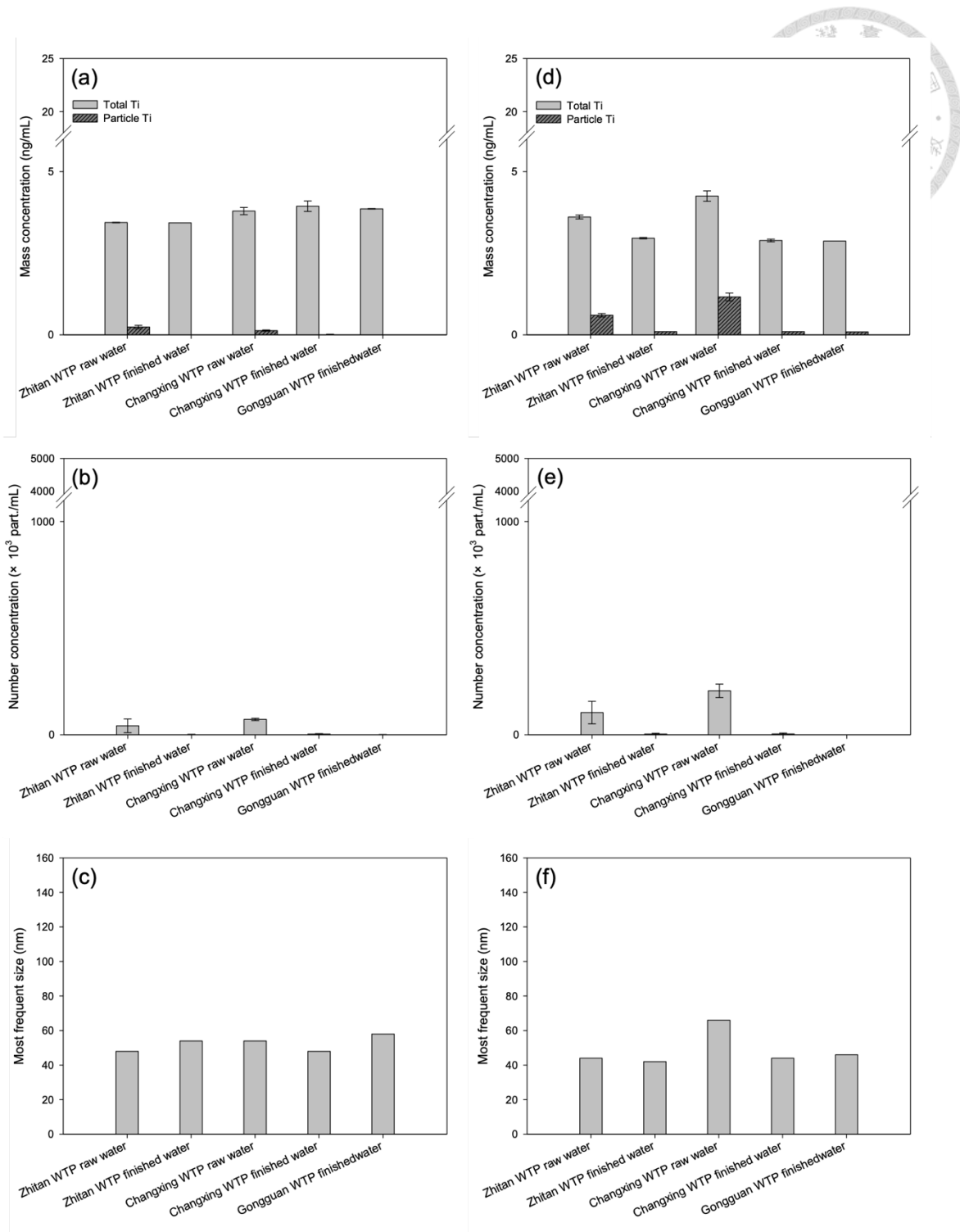


Fig. 4-5 Total Ti and particle Ti mass concentration (a,d), number concentration (b,e), and the most frequent size (c,f) of Ti-containing nanoparticles in the raw water and finished water from the Zhitan, Changxing, and Gongguan WTP.

### 4.2.3 Drinking water from the Dahan River and its tributary

#### 1. Total mass concentration

During the dry season, the total Ti concentration in raw water was  $11.0 \pm 0.12$  ng/mL and increased to  $12.3 \pm 0.03$  ng/mL in finished water. The opposite change in the total Ti concentration after water treatment was observed during the wet season. The total Ti levels in raw water and finished water were  $19.7 \pm 0.13$  ng/mL and  $4.92 \pm 0.12$  ng/mL, respectively, showing a significant decrease after water treatment processes.

#### 2. Particle mass concentration

The mass concentration of Ti containing particles in raw water was  $0.66 \pm 0.04$  ng/mL during the dry season, and water treatment processes eliminated about 95% of the particles, reducing the concentration in finished water to  $0.03 \pm 0.01$  ng/mL. The removal efficiency during the wet season was found to be 97%, slightly higher than that in the dry season, and the mass concentration of Ti containing particles was  $13.1 \pm 0.18$  ng/mL and  $0.40 \pm 0.01$  ng/mL in raw water and finished water, respectively.

#### 3. Number concentration

The decrease in number concentration of Ti containing particles after water treatment was observed in both the dry and wet season. The number concentration in raw water was  $90.9 \pm 14.8 \times 10^3$  part./mL and decreased to  $25.6 \pm 9.82 \times 10^3$  part./mL in finished water during the dry season. By comparing Fig. 4-6-(b) and (e), it can be seen that during the wet season, the number concentration of Ti containing particles had a larger decrease after water treatment, from  $3917 \pm 138 \times 10^3$  part./mL to  $260 \pm 37.5 \times 10^3$  part./mL, but the concentration level in finished water was still significantly higher.

#### 4. Most frequent size

During the dry season, the most frequent size of Ti-containing particles in raw water was 56 nm. After water treatment, the most frequent size of Ti-containing particles in finished water decreased to 52 nm. The opposite variation trend was observed in the wet season (Fig. 4-6-(f)). The most frequent size of Ti-containing particles in raw water was 36 nm, and significantly increased to 52 nm in finished water (Table 4-10).

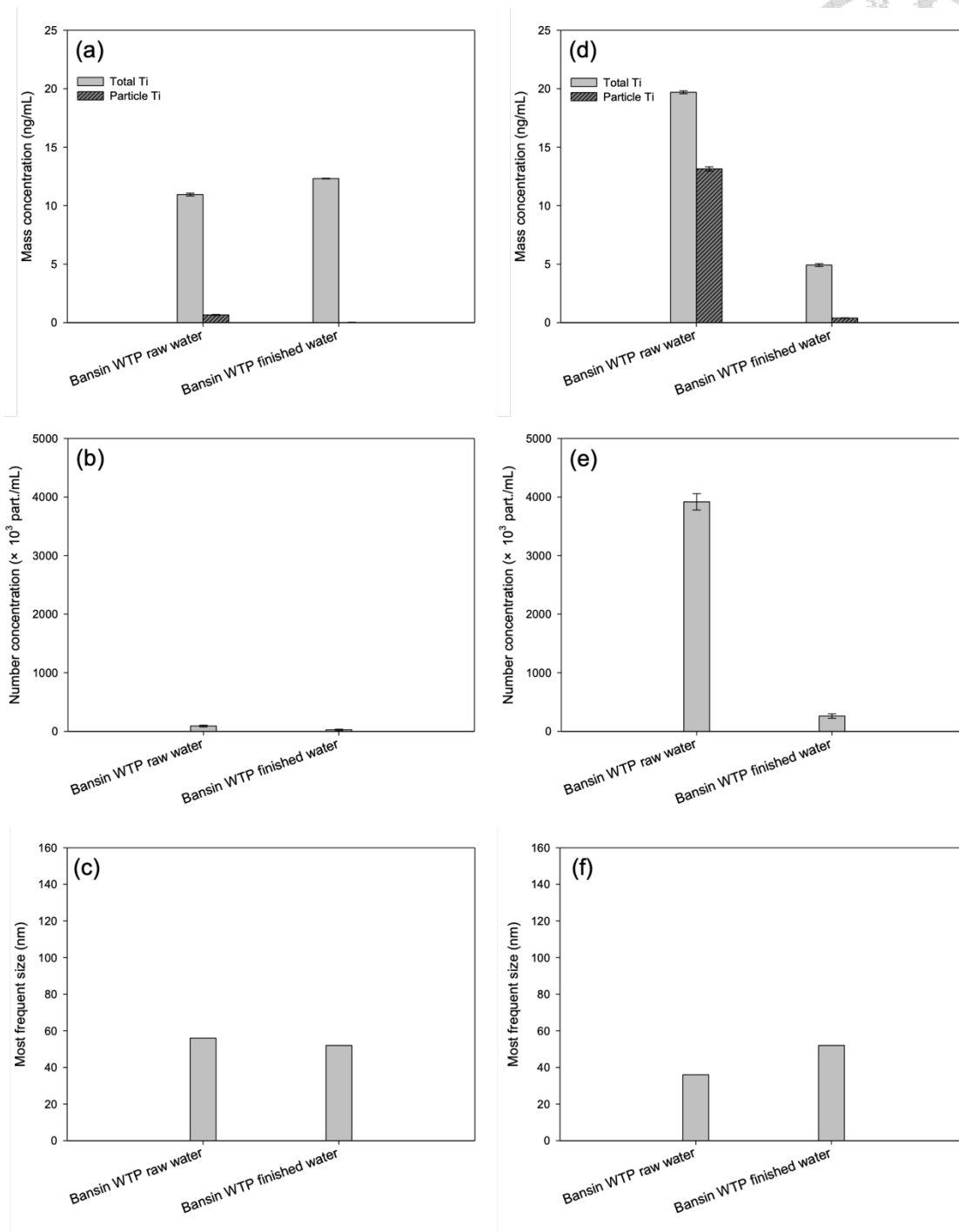


Fig. 4-6 Total Ti and particle Ti mass concentration (a,d), number concentration (b,e), and the most frequent size (c,f) of Ti-containing nanoparticles in the raw water and finished water from the Bansin WTP.

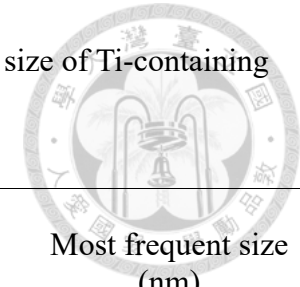


Table 4-10. Total Ti mass concentration, particle Ti mass concentration, number concentration and the most frequent size of Ti-containing nanoparticles in raw water and finished water.

	N	Total mass concentration (ng/mL) M ± SD	Particle mass concentration (ng/mL) M ± SD	Number concentration (×10 <sup>3</sup> part./mL) M ± SD	Most frequent size (nm)
<b>Dry season</b>					
<b>Xinshan WTP</b>					
Raw water	2	10.2 ± 0.85	1.45 ± 0.13	424 ± 14.5	32
Finished water	2	7.00 ± 0.07	0.09 ± 0.00	7.59 ± 0.29	48
<b>Zhitian WTP</b>					
Raw water	2	3.44 ± 0.01	0.24 ± 0.05	42.1 ± 31.0	48
Finished water	2	3.43 ± 0.00	0.01 ± 0.00	1.33 ± 1.04	54
<b>Changxing WTP</b>					
Raw water	2	3.79 ± 0.11	0.13 ± 0.02	72.1 ± 5.43	54
Finished water	2	3.94 ± 0.16	0.01 ± 0.01	3.54 ± 2.10	48
<b>Gongguan WTP</b>					
Finished water	2	3.86 ± 0.01	0.01 ± 0.00	1.03 ± 0.21	58

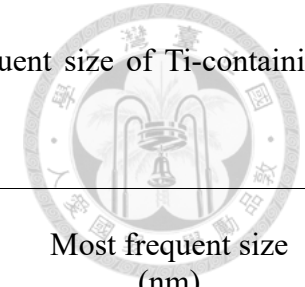


Table 4-10. Total Ti mass concentration, particle Ti mass concentration, number concentration and the most frequent size of Ti-containing nanoparticles in raw water and finished water (continued).

	N	Total mass concentration (ng/mL) M ± SD	Particle mass concentration (ng/mL) M ± SD	Number concentration (×10 <sup>3</sup> part./mL) M ± SD	Most frequent size (nm)
<b>Bansin WTP</b>					
Raw water	2	11.0 ± 0.12	0.66 ± 0.04	90.9 ± 14.8	56
Finished water	2	12.3 ± 0.03	0.03 ± 0.01	25.6 ± 9.82	52
<b>Wet season</b>					
<b>Xinshan WTP</b>					
Raw water	2	17.4 ± 0.87	10.1 ± 0.64	3262 ± 172	42
Finished water	2	3.40 ± 0.07	0.14 ± 0.06	105 ± 114	44
<b>Zhitian WTP</b>					
Raw water	2	3.61 ± 0.06	0.60 ± 0.05	104 ± 52.6	44
Finished water	2	2.96 ± 0.02	0.10 ± 0.00	3.51 ± 3.80	42
<b>Changxing WTP</b>					
Raw water	2	4.25 ± 0.16	1.16 ± 0.12	206 ± 31.6	66
Finished water	2	2.89 ± 0.04	0.10 ± 0.00	3.93 ± 4.38	44

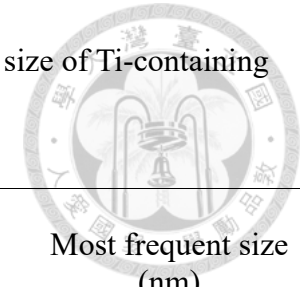


Table 4-10. Total Ti mass concentration, particle Ti mass concentration, number concentration and the most frequent size of Ti-containing nanoparticles in raw water and finished water (continued).

	N	Total mass concentration (ng/mL) M ± SD	Particle mass concentration (ng/mL) M ± SD	Number concentration (×10 <sup>3</sup> part./mL) M ± SD	Most frequent size (nm)
<b>Gongguan WTP</b>					
Finished water	2	2.87 ± 0.00	0.09 ± 0.00	0.41 ± 0.00	46
<b>Bansin WTP</b>					
Raw water	2	19.7 ± 0.13	13.1 ± 0.18	3917 ± 138	36
Finished water	2	4.92 ± 0.12	0.40 ± 0.01	260 ± 37.5	52

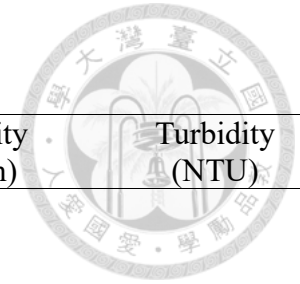


Table 4-11. Water quality parameters of raw water and finished water.

	Temperature (°C)	pH	Conductivity ( $\mu$ S/cm)	TDS (mg/L)	Salinity (ppm)	Turbidity (NTU)
<b>Dry season</b>						
<b>Xinshan WTP</b>						
Raw water	18.2	7.49	192.0	173.0	90.5	6.85
Finished water	18.6	7.05	205.0	185.0	96.0	0.32
<b>Zhitai WTP</b>						
Raw water	19.8	7.46	88.6	79.7	41.9	2.28
Finished water	21.3	7.29	92.3	83.1	44.0	0.19
<b>Changxing WTP</b>						
Raw water	20.8	7.48	92.2	83.0	43.0	2.89
Finished water	21.6	7.53	99.9	89.9	46.7	0.19
<b>Gongguan WTP</b>						
Finished water	20.7	7.53	102.1	91.9	48.0	0.23
<b>Bansin WTP</b>						
Raw water	21.6	8.94	197.5	175.8	92.8	6.63
Finished water	21.1	7.59	236.0	212.4	115.0	1.89

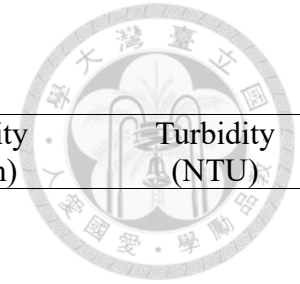


Table 4-11. Water quality parameters of raw water and finished water (continued).

	Temperature (°C)	pH	Conductivity ( $\mu$ S/cm)	TDS (mg/L)	Salinity (ppm)	Turbidity (NTU)
<b>Wet season</b>						
<b>Xinshan WTP</b>						
Raw water	27.1	7.49	114.1	102.2	53.2	45.3
Finished water	26.0	7.13	121.8	110.0	57.7	0.35
<b>Zhitai WTP</b>						
Raw water	24.1	7.47	84.7	75.9	39.2	7.15
Finished water	24.0	7.13	79.5	71.4	37.3	0.20
<b>Changxing WTP</b>						
Raw water	23.4	7.44	82.8	74.3	38.7	7.15
Finished water	24.2	7.37	85.3	76.6	39.9	0.23
<b>Gongguan WTP</b>						
Finished water	23.3	7.31	89.6	80.0	41.5	0.78
<b>Bansin WTP</b>						
Raw water	24.9	7.86	128.9	115.4	58.1	27.7
Finished water	25.5	7.24	129.7	116.3	60.6	1.66

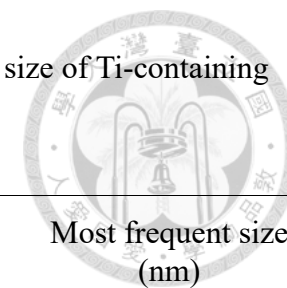


Table 4-12. Total Ti mass concentration, particle Ti mass concentration, number concentration and the most frequent size of Ti-containing nanoparticles in water treatment plant field blanks.

	N	Total mass concentration (ng/mL)	Particle mass concentration (ng/mL)	Number concentration ( $\times 10^3$ part./mL)	Most frequent size (nm)
<b>Dry season</b>					
<b>Keelung River</b>					
Xinshan WTP	1	0.26	0.08	0.82	36
<b>Xindian River</b>					
Zhitan WTP	1	0.06	0.01	0.89	44
Changxing WTP	1	0.05	0.01	1.48	38
Gongguan WTP	1	0.16	0.01	0.89	50
<b>Dahan River</b>					
Bansin WTP	1	0.17	0.01	1.18	32

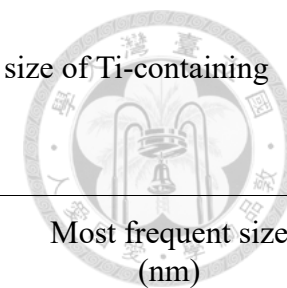


Table 4-12. Total Ti mass concentration, particle Ti mass concentration, number concentration and the most frequent size of Ti-containing nanoparticles in water treatment plant field blanks (continued).

	N	Total mass concentration (ng/mL)	Particle mass concentration (ng/mL)	Number concentration ( $\times 10^3$ part./mL)	Most frequent size (nm)
<b>Wet season</b>					
<b>Keelung River</b>					
Xinshan WTP	1	0.10	0.10	20.7	28
<b>Xindian River</b>					
Zhitan WTP	1	0.19	0.21	2.07	28
Changxing WTP	1	0.06	0.10	2.89	28
Gongguan WTP	1	0.11	0.12	2.07	30
<b>Dahan River</b>					
Bansin WTP	1	0.36	0.26	0.89	38

## Chapter 5 Discussion



### 5.1 Detection of Ti containing particles in the water sources of the Greater Taipei area

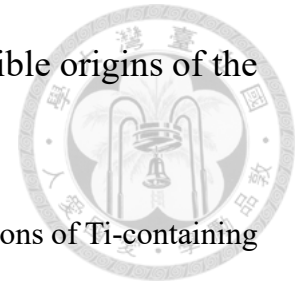
#### 5.1.1 Comparison with previous studies in mass concentration, number concentration, and particle size

In this study, we obtained quantitative information on Ti-containing nanoparticles in rivers that supply the Greater Taipei area, including mass concentration, number concentration, and the most frequent size. The mass concentration of all samples was higher than the detection limit (10.47 ng/L), and the dissolved Ti background of each sample allowed Ti-containing particles larger than around 20 nm to be stably detected. The mass concentration of Ti-containing particles varied among the studied rivers and have noticeable temporal changes, but overall, the mass concentration range in drinking water sources ranged from 0.05 to 11.29 ng/mL. These values were one order of magnitude higher or lower than the model-predicted concentrations of TiO<sub>2</sub> nanoparticles in surface water reported mainly in Europe and the United States (Gottschalk *et al.*, 2009; Tiede *et al.*, 2016). These findings suggested that, in our study area, typical model inputs such as production, application volume, and, more notably, the environmental fate of engineered TiO<sub>2</sub> were somewhat different from those set in those previous studies. Besides, these modelling studies only predicted the concentration of engineered TiO<sub>2</sub> nanoparticles, but did not consider the background concentration caused by naturally and incidentally occurring Ti-containing particles. Based on the findings in our study, it could be concluded that the contribution of naturally occurring Ti-containing particles was quite

significant, which will be further elaborated on in the following sections.

Recently, the sp-ICPMS has been widely applied to the analysis of environmental water for further information on Ti-containing particles such as number concentration and particle size in addition to mass concentration. The findings of this study were similar to several previous experimental studies in terms of mass concentration, ranging from low to sub- $\mu\text{g/L}$  with a relatively wide distribution. Such wide variation might have resulted from the measurements covering three river systems, which feature different hydrological and seasonal characteristics. However, even with similar mass concentration ranges, we found a comparatively high number concentration of Ti-containing particles in the present study. The highest detected number concentration ( $4109 \times 10^3 \text{ part./mL}$ ) in the Keelung River was one to two orders of magnitude higher than previously reported values (Gondikas *et al.*, 2014; Peters *et al.*, 2018). The size range of the Ti-containing particles we found also seemed to differ from those of previous studies. In this study, the most frequent sizes of Ti-containing particles measured in all river water samples were between 36 nm and 76 nm, while most previous studies reported that the size of  $\text{TiO}_2$  particles present in surface water fell within the range from hundreds nanometer to micrometer. There are many possible explanations for the inconsistency of the number concentration and the particle size range across different studies, such as diverse origins, transformations modified by the physical and chemical properties of the surrounding medium when the Ti-containing particles enter the river, and the sample pretreatment method for Ti determination, etc.

### 5.1.2 Spatial distribution of mass concentration and possible origins of the Ti-containing particles



Generally, the total mass, particle mass, and number concentrations of Ti-containing particles in all studied rivers showed a similar spatial trend to steadily increase downstream. This indicates that there were stable and continuous reception and accumulation of Ti-containing particles in downstream rivers, in most cases the increase in concentration likely originated from diffuse sources. An exceptional point release was suspected to occur along the Keelung River during the sampling period in the wet season. We observed an abrupt increase in both total Ti concentration and mass concentration of Ti-containing particles at the Badu Pumping Station (Fig. 4-1-(a)), and the noticeable increase in turbidity (Table 4-2) may be used to support that there was a released source between the Jieshou Bridge and the Badu Pumping Station. Factories in the upstream Ruifang Industrial Park located upstream of the Keelung River, occasionally discharge industrial wastewater containing heavy metals and other unknown pollutants into the Keelung River along with rainwater, which is a potential source of Ti.

Considerable differences in Ti-containing particles concentration occur among rivers. In general, the Dahan River System has the highest levels of both total Ti concentration and Ti-containing particle mass concentration, followed by the Keelung River and then the Xindian River. A possible explanation for this lies in regional geological differences. Fe-Ti oxide minerals are often found in igneous rocks. In northern Taiwan, it was reported that Fe-Ti oxide minerals appear in the Chilung volcano group and in the vicinity of the Shimen Reservoir (陳正宏, 1990). Because mineral weathering and biological processes (e.g., redox reaction driven by aqueous bacterial) release ions and usually also produce nano-scale minerals (Hochella *et al.*, 2008), this may lead to the relatively high natural

background of both ionic Ti and Ti-containing particles in the Keelung River and the Dahan River Systems.

In addition to natural geologic factors, we found that land-use types could also be used to explain the varying levels of Ti-containing particles in the three studied rivers. It has been recognized that architectural coatings and white road markings contain TiO<sub>2</sub> pigments that release nano-to-micron size engineered TiO<sub>2</sub> particles during the weathering process (Al-Kattan *et al.*, 2013; Kaegi *et al.*, 2008; Wang *et al.*, 2020), likely causing built-up areas to become diffuse sources of engineered TiO<sub>2</sub> particles. The transportation, construction, public, and recreational land use in the riparian area of the study rivers is represented graphically in Fig 5-1. It can be seen that the Dahan River System and the Keelung River, with relatively high total Ti and mass concentration of Ti-containing particles, have a significantly higher proportion of built-up land use in riparian areas than in the Xindian River System. This supports that urban runoff is likely to be an important source of Ti-containing particles in the receiving river, and a certain portion of the detected Ti-containing particles is engineered TiO<sub>2</sub> released by industrial paints.

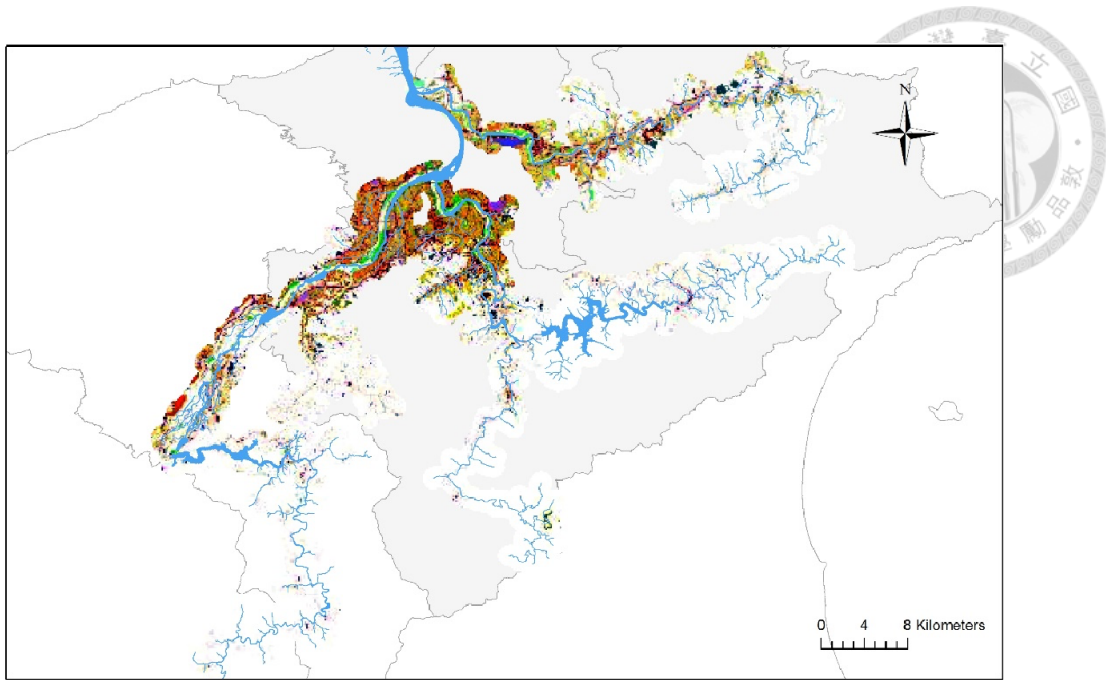


Fig. 5-1 Map of built-up land use of the riparian area within one kilometer of the Keelung River, Xindian River, and Dahan River.

Past studies have regarded domestic wastewater as one of the main sources of engineered nanoparticles into surface water, and it has been confirmed that Ti-containing particles are present in treated wastewater (Kiser *et al.*, 2009) and an increase in number concentration has been observed in the receiving river around the wastewater outlet (Phalyvong *et al.*, 2020). In this study, extra samples were collected downstream from the effluent outfall of the Wulai and Zhitan sewage treatment plants (shown in Fig. 5-2) during the wet season. As shown in Table 5-1, all the concentration values of the extra samples are higher than the overall level of Xindian River in the dry season. While compared with other samples collected upstream, no significant increase or variation in all the analysis values was observed as expected. This implied that the contribution of domestic wastewater effluent to the concentration of Ti-containing particles may be relatively limited and there must be other more significant sources. There was also a study which did not detect an increase in the concentration of Ti around the effluent outfall. The

results were attributed to the fact that because 90% of Ti can be effectively removed through wastewater treatment the treated effluent showed significantly lower than the predicted concentrations previously reported (Markus *et al.*, 2018). Since this study did not analyze the wastewater effluent, the rapid aggregation and settlement of part of the Ti-containing particles in the effluent (Velzeboer *et al.*, 2014), or the dilution effect during the wet season all of which may also cause the contribution of wastewater effluent to become less significant. The conductivity, TDS, and salinity values of all the rivers investigated in this study were significantly lower than the corresponding values during the dry season, which supports that the river water has been diluted by rainfall during the sampling period. Shi *et al.* also even measured lower Ti concentration in wastewater than in the receiving river and further concluded that there are other more important sources of Ti than wastewater effluent, such as urban runoff (Shi *et al.*, 2016), which is similar to our presumption for natural Ti releasing sources. However, it is difficult to identify the possible main source of Ti-containing particles in this study, because it is unachievable to differentiate between natural and engineered Ti-containing particles due to the lack of natural background information on Ti concentration in rivers and the limitation of sp-ICPMS analysis.

Table 5-1. The total Ti mass concentration, particle Ti mass concentration, number concentration and most frequent size of the Ti-containing particles in the river water samples downstream of the sewage treatment outfall.

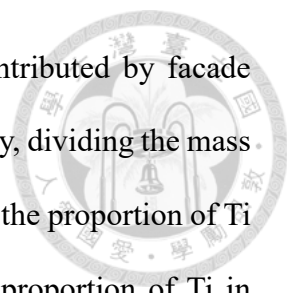
	Total mass concentration (ng/mL) M ± SD	Particle mass concentration (ng/mL) M ± SD	Number concentration (×10 <sup>3</sup> part./mL) M ± SD	Most frequent size (nm)
Yangguan Bridge (N=2)	4.20 ± 0.01	0.97 ± 0.05	268 ± 31.8	48



Fig. 5-2 Map of the sampling site downstream from the sewage treatment outfall.

### 5.1.3 Seasonal changes, possible causes, in mass concentration

In all rivers, the total concentration, mass concentration, and number concentration of Ti-containing particles all presented consistent seasonal changes, with significant increases during the wet season, which suggests there was a relationship between rainfall and the occurrence of Ti-containing particles in rivers. Rainwater could be a source of Ti-containing particles due to the abundance of Ti in the environment. The reported total Ti concentration in rainwater ranged from 1 to 10  $\mu\text{g/L}$  (Hu and Balasubramanian, 2003). Heimbürger et al. further discovered the low solubility of Ti among all metals in rainwater and pointed out that the insoluble fraction of Ti increases when receiving pollutant emissions (Heimbürger *et al.*, 2013). As mentioned earlier, architectural paints and road markings release  $\text{TiO}_2$  particles causing the rainwater runoff from the facades to contain  $\text{TiO}_2$  particles, and the released amount would be associated with the intensity of



precipitation, thus suggesting that the amount of  $\text{TiO}_2$  particles contributed by facade runoff would also increase during the wet season. For the present study, dividing the mass concentration of Ti-containing particles by the total Ti concentration, the proportion of Ti in particulate form in rivers was obtained. It can be seen that the proportion of Ti in particulate form in all river samples was significantly higher during the wet season, indicating that the increase in Ti in the wet season is mostly in the form of particles, which may also be related to rainfall. Rainfall is known to increase confluence, and the increase in river flow during the wet season sampling period in this study is also confirmed (經濟部水利署, 2020). Previous studies have pointed out that Ti in river water is mainly associated with suspended solids and sediments because Ti has a relatively high partition coefficient between solid and dissolved fraction (Roychoudhury and Starke, 2006; Veselý *et al.*, 2001). Accordingly, the increase in the concentration of Ti particles in river water during the wet season is most likely due to the higher river flow that intensifies subsequent riverbed erosion and resuspension of sediments. This also explains why, in most cases, the temporal variation and spatial distribution trend of the concentration of Ti-containing particles correspond to that of turbidity in rivers (Fig. 5-3).

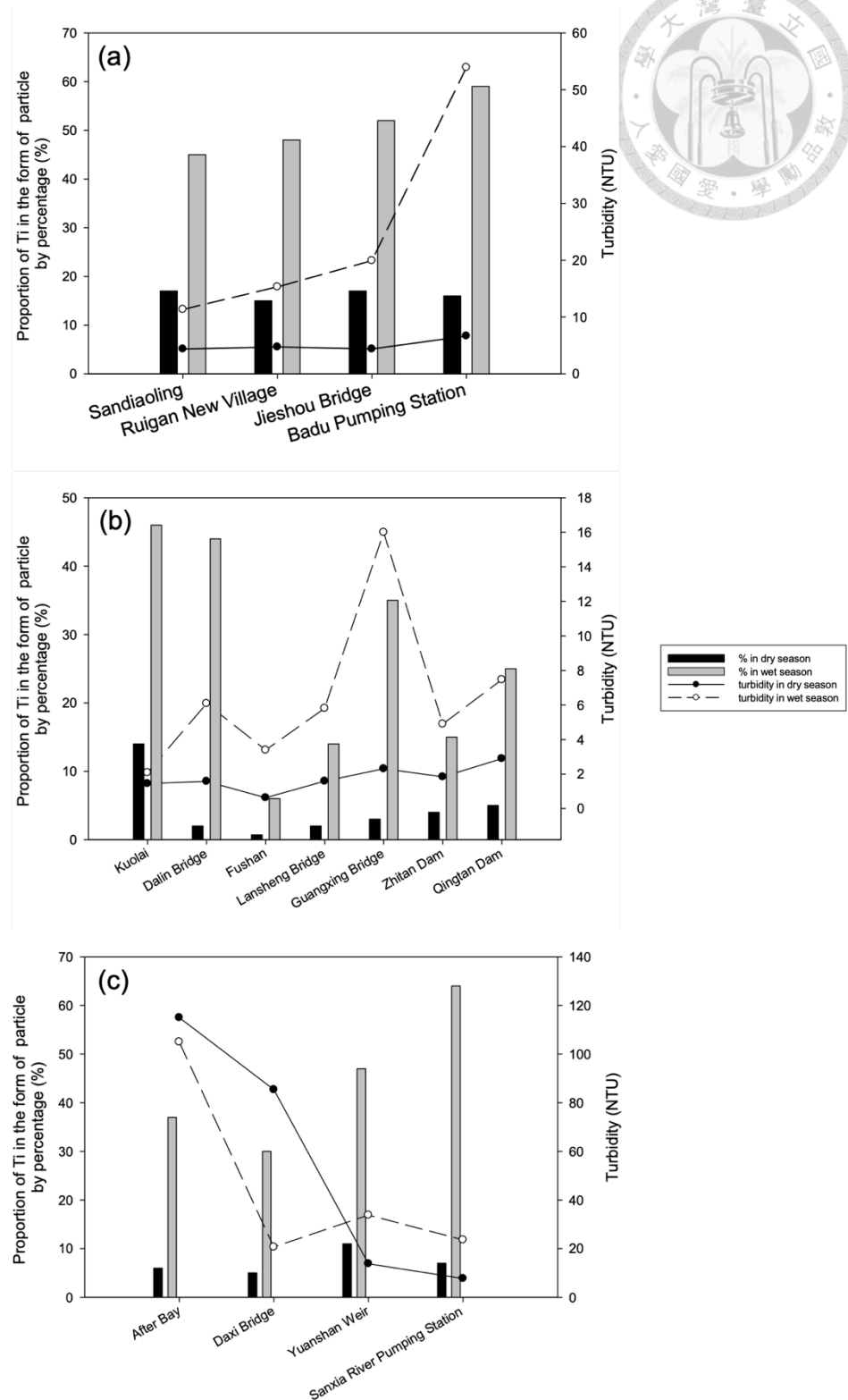


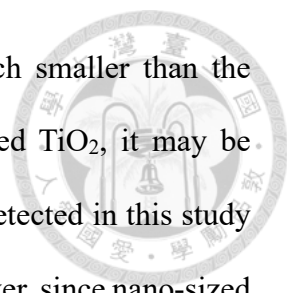
Fig. 5-3 Proportion of Ti in the form of particle by percentage (%) and turbidity (NTU) in samples from (a) Keelung River, (b) Xindian River, and (c) Dahan River, respectively, in both dry and wet season.

#### 5.1.4 Possible factors affecting particle sizes

The results of several previous studies have shown that sp-ICPMS is not a consistently effective technique for detecting nanoparticles in environmental water (Gondikas *et al.*, 2014; Peters *et al.*, 2018). High ionic Ti background or isotope (e.g.,  $^{48}\text{Ca}$ ) interference can cause failure to detect nano-sized Ti-containing particles. Nevertheless, in this study, Ti-containing particles smaller than 100 nm were successfully measured in all river samples, showing that sp-ICPMS is a suitable method for monitoring the level of Ti-containing particles in water sources of the Greater Taipei area.

In addition to being confirmed to exist in water sources, nano-sized Ti-containing particles were found to account for the majority of Ti in water samples. Such particle size was much smaller than the reported size range in surface water (Gondikas *et al.*, 2014; Peters *et al.*, 2018; Phalyvong *et al.*, 2020). There is concern that when filtration is used as pretreatment method, the electrostatic attraction and repulsion that occurs on the surface of the filter membrane may cause clogging and high-efficiency interception of nanoparticles (Yang *et al.*, 2016), thus causing the particles that can pass through the filter to be much smaller than the stated pore size. However, considering that the extent of interception is related to nanoparticle concentration (Ullmann *et al.*, 2019), in this study, filtration may have a relatively minor effect on samples with such a low concentration.

Particle sizes of engineered  $\text{TiO}_2$  in the environment are expected to be comparable to that in common consumer products. Taking food-grade additives and paint pigments as examples, they both contain primary particle sizes which can range from nano range to hundreds of nanometers, mainly around 100 nm and between 100 to 300 nm, respectively (Loosli *et al.*, 2019; Weir *et al.*, 2012). Moreover, these particles tend to exist in water as larger aggregates, especially in rivers, because the turbulence increases particle collision frequency thus enhancing and accelerating aggregation (Velzeboer *et al.*,



2014). Based on the fact that the measured particle size was much smaller than the expected size of the primary particles and aggregates of engineered TiO<sub>2</sub>, it may be presumed that the main composition of the Ti-containing particles detected in this study was not directly derived from common industrial applications. However, since nano-sized particles may be separated from larger aggregates and resuspended due to hydraulic organization in rivers (Oliveira *et al.*, 2019), it may not be possible to exclude the contribution of anthropogenic sources solely based on the particle size. For such low concentration and small size distribution of Ti-containing particles as in this study, using element ratios to determine the origin may be a feasible method (Gondikas *et al.*, 2014; Phalyvong *et al.*, 2020; Wang *et al.*, 2020). However, this requires an understanding of the composition of other elements (commonly used elements such as Al, Fe, Nb, etc.) in naturally occurring particles. Future study is warranted to establish relevant regional background information in advance.

It is also worth noting that unlike the apparent spatial and seasonal trends observed in concentration, the particle size of Ti-containing particles was relatively uniform and shows only minor fluctuations. One possibility is that the surrounding medium conditions that determine the stability of Ti-containing particles, such as pH, did not have much variation among all sampling points and sampling periods in different seasons. Also, particle size is a feature that is known to be associated with the distribution of particles in rivers. In the Danshui River, which the lower reaches of the confluence of the rivers was investigated in this study, it was reported that the size of suspended sediments vertically increases in relation to water depth (林柏青 *et al.*, 2014). Since the samples in this study were collected from fixed sampling locations at similar water depths, comparable hydrodynamic conditions might therefore cause the Ti-containing particles in the samples to have relatively uniform and constant sizes. However, such interpretation will still

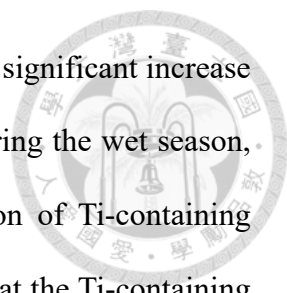
require further study to collect necessary information for verification.



## 5.2 Ti-containing particles in drinking water

In this study, the analysis results of the finished water samples may represent the potential exposure of Ti-containing particles for approximately 84% of tap water users in the Greater Taipei area. The overall range of mass concentration and number concentration of Ti-containing particles remaining in finished water was between 0.01 to 0.40 ng/mL and 1.03 to  $260 \times 10^3$  part./mL, respectively. At present, there are still very few experimental studies on the concentration of Ti-containing particles in tap water. Another relevant study was carried out by Yang et al. and the mass concentration and number concentration of Ti-containing particles in tap water in the US was reported to be 3.1ng/L and  $7.54 \times 10^2$  part./mL, both of which were lower than the corresponding values found in the present study (Yang and Westerhoff, 2014). We concluded that the concentration level of Ti-containing particles in tap water is mainly determined by the characteristic of the water source, which is supported by the analysis results and discussed in details below.

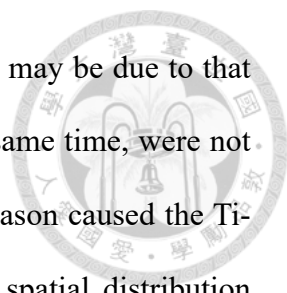
Both the mass concentration and number concentration of Ti-containing particles consistently show a significant decrease after being treated in WTPs. The Ti-containing particle removal efficiency of conventional water treatment process found in this study ranged from 83% to 99% and exceeded 90% in most situations, which is in line with previously reported laboratory simulations (Honda *et al.*, 2014; Kinsinger *et al.*, 2015; Sousa and Ribau Teixeira, 2020). As described in section 4.2.2, the removal efficiency measured at the Changxing and Gongguan WTPs was almost constant. Similarly, the seasonal variation in the concentration of Ti-containing particles and the turbidity of the



shared raw water were also relatively insignificant (Table 4-11). The significant increase in removal efficiency occurred in the Xinshan and Banxin WTP during the wet season, and the consistency is the substantial increase in the concentration of Ti-containing particles and turbidity of the raw water. The above results suggest that the Ti-containing particle concentration and turbidity of the raw water may be important characteristics that affect the removal efficiency. This is reasonable because the higher concentration of particulate matter in raw water increases the frequency of collisions of particles and thus enhances coagulation (Honda *et al.*, 2014). Also, to meet drinking water standards, a higher coagulant dosage may be added due to the increase in raw water turbidity, which may also lead to the enhanced removal rate of Ti-containing particles.

Another noteworthy finding is that the removal efficiency of the Gongguan WTP was found approximately equivalent to that of Changxing WTP in both wet and dry seasons sampling periods. In addition to sharing the raw water, part of the raw water was transported to the Gongguan WTP after coagulant was added at the Changxing WTP, and the subsequent treatment procedure was completed separately. This suggests that the coagulation stage may have a relatively huge impact on the removal of Ti-containing particles compared to other treatment procedures. Sweep flocculation has been pointed out as the main mechanism for removing Ti-containing particles in conventional water treatment (Honda *et al.*, 2014; Sousa and Ribau Teixeira, 2020), and the results mentioned above are also consistent with this view.

We found an exception at the Zhitan WTP that its removal efficiency did not show a similar increasing trend as expected as Ti-containing particles concentration and turbidity in raw water. It can be found that in the dry season, due to the proximity of the water intake, the raw water of the Zhitan and Changxing WTPs have similar Ti-containing particle levels. In contrast, the concentration found in the Zhitan WTP in the wet season



was significantly lower than at the Changxing WTP. This difference may be due to that raw water and finished water samples, although collected from the same time, were not from the same batch, and the short-duration of rainfall in the wet season caused the Ti-containing particles in the source river to be more likely to have spatial distribution fluctuations. Accordingly, to avoid the interference of rainfall in evaluating the Ti-containing particles removal efficiency of the water treatment, future studies should consider processing time to collect more representative samples. Also, since the concentration of Ti-containing particles in finished water may vary closely with the concentration of raw water, it may be necessary to increase the sampling frequency especially during the wet season.

At present, there is no standard for the concentration of Ti-containing particles in drinking water. The only regulation on the concentration of Ti-containing particles in the intake through digestion is the regulation of TiO<sub>2</sub> as an additive to food, medicine or cosmetics. In the United States, TiO<sub>2</sub> is restricted to be less than 1% by weight of food when used as a food colorant (21 CFR 73.575), while in EU countries no relevant restriction was established. Under such conditions the maximum exposure for adults is believed to be 20 mg/kg bw/day (Jovanović *et al.*, 2018). In this study, given that the average daily drinking water intake for adults in Taiwan is about 1.43 L/day (行政院衛生署, 2008), it is estimated that potential Ti-containing particles intake through drinking water ranges from 14 to 573 ng/day. Due to the lack of established acceptable daily intake standards, levels of exposure over a long-term period has not yet been guaranteed to be acceptable, but it can be observed that drinking water may be a relatively less significant source for ingestion of Ti-containing particles in comparison to other sources. However, since TiO<sub>2</sub> has been banned as a food additive in France, which was followed by other

countries, and there has been a significant increase in TiO<sub>2</sub> application in other fields. Drinking water may gradually become an important source of oral exposure to Ti-containing nanoparticles for the general public in the future. Therefore, continuous monitoring of the concentration of Ti-containing particles in drinking water is still necessary.

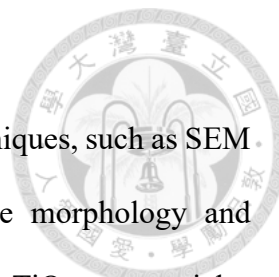
## Chapter 6 Conclusions



1. The mass concentration, number concentration, and most frequent size ranges of Ti-containing particles were 1.14–11.5 ng/mL, 170–4110 $\times 10^3$  part./ml, 36–42 nm in the Keelung River, and 0.72–12.2 ng/mL, 108–4162  $\times 10^3$  part./ml, 38–76 nm in the Dahan River system. The Xindian River system had the lowest level of Ti-containing particles among the three river systems investigated in this study. The mass concentration, number concentration, and particle size range of Ti-containing particles were 0.05–1.92 ng/mL, 5.32–417  $\times 10^3$  part./ml, and 38–66 nm.
2. The longitudinal distribution of Ti-containing particles in the studied rivers gives an indication that the Ti-containing particles were mainly derived from diffusion sources. The higher concentration of Ti-containing particles in the Keelung River and the Dahan River Systems may be related to the regional geological composition and the higher proportion of anthropogenic land use in the riparian area.
3. During the wet season, the concentration of Ti-containing particles in the studied rivers increased significantly, demonstrating the important influence of rainfall on the occurrence or release of Ti-containing particles.
4. Ti-containing particles' removal efficiency through conventional water treatment was discovered to be between 83% and 99%. The concentration of particulate matter in the raw water might be an important characteristic that affects the removal efficiency. Given that the range of mass concentration, number concentration, and most frequent size of Ti-containing particles in finished water was 0.01–0.40 ng/mL, 1.03–260  $\times 10^3$  part./ml, and 32–66 nm, respectively, the potential Ti-containing nanoparticles intake through drinking water was estimated to be 14–573 ng/day

( $6-3,718 \times 10^5$  part./day).

5. It is recommended that future studies couple other analysis techniques, such as SEM and spICPTOFMS, to provide additional information on the morphology and element composition of individual particles to better differentiate TiO<sub>2</sub> nanoparticles from anthropogenic origins.



## REFERENCES



- Al-Kattan A, Wichser A, Vonbank R, Brunner S, Ulrich A, Zuin S, Nowack B. Release of TiO<sub>2</sub> from paints containing pigment-TiO<sub>2</sub> or nano-TiO<sub>2</sub> by weathering. *Environmental Science Processes & Impacts* 2013;**15**:2186-93. doi: 10.1039/c3em00331k.
- Auffan M, Rose J, Bottero J-Y, Lowry G, Jolivet J-P, Wiesner M. Towards a definition of inorganic nanoparticles from an environmental, health and safety perspective. *Nature Nanotechnology* 2009;**4**:634-41. doi: 10.1038/nano.2009.242.
- Baalousha M, Cornelis G, Kuhlbusch TAJ, Lynch I, Nickel C, Peijnenburg W, van den Brink NW. Modeling nanomaterial fate and uptake in the environment: current knowledge and future trends. *Environmental Science-Nano* 2016;**3**:323-45. doi: 10.1039/c5en00207a.
- Becker K, Schroecksadel S, Geisler S, Carriere M, Gostner JM, Schennach H, Herlin N, Fuchs D. TiO<sub>2</sub> nanoparticles and bulk material stimulate human peripheral blood mononuclear cells. *Food and Chemical Toxicology* 2014;**65**:63-9. doi: <https://doi.org/10.1016/j.fct.2013.12.018>.
- Benn TM, Westerhoff P. Nanoparticle silver released into water from commercially available sock fabrics. *Environmental Science & Technology* 2008;**42**:4133-9. doi: 10.1021/es7032718.
- Bossa N, Chaurand P, Levard C, Borschneck D, Miche H, Vicente J, Geantet C, Aguerre-Chariol O, Michel FM, Rose J. Environmental exposure to TiO<sub>2</sub> nanomaterials incorporated in building material. *Environmental Pollution* 2017;**220**:1160-70. doi: 10.1016/j.envpol.2016.11.019.
- Chalew Talia EA, Ajmani Gaurav S, Huang H, Schwab Kellogg J. Evaluating nanoparticle breakthrough during drinking water treatment. *Environmental Health Perspectives* 2013;**121**:1161-6. doi: 10.1289/ehp.1306574.
- Crosera M, Prodi A, Mauro M, Pelin M, Florio C, Bellomo F, Adami G, Apostoli P, De Palma G, Bovenzi M, Campanini M, Filon FL. Titanium dioxide nanoparticle penetration into the skin and effects on HaCaT cells. *Int J Environ Res Public Health* 2015;**12**:9282-97. doi: 10.3390/ijerph120809282.
- Donovan AR, Adams CD, Ma Y, Stephan C, Eichholz T, Shi H. Single particle ICP-MS characterization of titanium dioxide, silver, and gold nanoparticles during drinking water treatment. *Chemosphere* 2016;**144**:148-53. doi: 10.1016/j.chemosphere.2015.07.081.
- Fabian E, Landsiedel R, Ma-Hock L, Wiench K, Wohlleben W, Van Ravenzwaay BJAot. Tissue distribution and toxicity of intravenously administered titanium dioxide

nanoparticles in rats. 2008;**82**:151-7.

Geraets L, Oomen AG, Krystek P, Jacobsen NR, Wallin H, Laurentie M, Verharen HW, Brandon EFA, de Jong WH. Tissue distribution and elimination after oral and intravenous administration of different titanium dioxide nanoparticles in rats. *Particle and Fibre Toxicology* 2014;**11**. doi: 10.1186/1743-8977-11-30.

Giese B, Klaessig F, Park B, Kaegi R, Steinfeldt M, Wigger H, von Gleich A, Gottschalk F. Risks, release and concentrations of engineered nanomaterial in the environment. *Scientific Reports* 2018;**8**:1565. doi: 10.1038/s41598-018-19275-4.

Gondikas AP, von der Kammer F, Reed RB, Wagner S, Ranville JF, Hofmann T. Release of TiO<sub>2</sub> nanoparticles from sunscreens into surface waters: A one-year survey at the Old Danube recreational lake. *Environmental Science & Technology* 2014;**48**:5415-22. doi: 10.1021/es405596y.

Gottschalk F, Nowack B. The release of engineered nanomaterials to the environment. *Journal of Environmental Monitoring* 2011;**13**:1145-55. doi: 10.1039/c0em00547a.

Gottschalk F, Sonderer T, Scholz RW, Nowack B. Modeled environmental concentrations of engineered nanomaterials (TiO<sub>2</sub>, ZnO, Ag, CNT, Fullerenes) for different regions. *Environmental Science & Technology* 2009;**43**:9216-22. doi: 10.1021/es9015553.

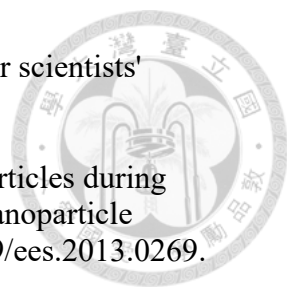
Gottschalk F, Sun T, Nowack B. Environmental concentrations of engineered nanomaterials: Review of modeling and analytical studies. *Environmental Pollution* 2013;**181**:287-300. doi: 10.1016/j.envpol.2013.06.003.

Heimbürger A, Losno R, Triquet S. Solubility of iron and other trace elements in rainwater collected on the Kerguelen Islands (South Indian Ocean). *Biogeosciences* 2013;**10**:6617-28. doi: 10.5194/bg-10-6617-2013.

Heringa MB, Peters RJB, Bleys R, van der Lee MK, Tromp PC, van Kesteren PCE, van Eijkeren JCH, Undas AK, Oomen AG, Bouwmeester H. Detection of titanium particles in human liver and spleen and possible health implications. *Part Fibre Toxicol* 2018;**15**:15. doi: 10.1186/s12989-018-0251-7.

Hochella MF, Jr., Lower SK, Maurice PA, Penn RL, Sahai N, Sparks DL, Twining BS. Nanominerals, mineral nanoparticles, and earth systems. *Science* 2008;**319**:1631-5. doi: 10.1126/science.1141134.

Hochella MF, Mogk DW, Ranville J, Allen IC, Luther GW, Marr LC, McGrail BP, Murayama M, Qafoku NP, Rosso KM, Sahai N, Schroeder PA, Vikesland P, Westerhoff P, Yang Y. Natural, incidental, and engineered nanomaterials and their impacts on the Earth system. *Science* 2019;**363**:eaau8299. doi: 10.1126/science.aau8299.

- 
- Hochella MF, Spencer MG, Jones K. Nanotechnology: nature's gift or scientists' brainchild? 2015;**2**:114-9.
- Honda RJ, Keene V, Daniels L, Walker SL. Removal of TiO<sub>2</sub> nanoparticles during primary water treatment: Role of coagulant type, dose, and nanoparticle concentration. *Environ Eng Sci* 2014;**31**:127-34. doi: 10.1089/ees.2013.0269.
- Hu GP, Balasubramanian R. Wet deposition of trace metals in Singapore. *Water, Air, and Soil Pollution* 2003;**144**:285-300. doi: 10.1023/A:1022921418383.
- Inshakova E, Inshakov OJMWC. World market for nanomaterials: structure and trends. 2017;**129**:02013.
- Jankovic NZ, Plata DL. Engineered nanomaterials in the context of global element cycles. *Environmental Science-Nano* 2019;**6**:2697-711. doi: 10.1039/c9en00322c.
- Jeevanandam J, Barhoum A, Chan YS, Dufresne A, Danquah MK. Review on nanoparticles and nanostructured materials: history, sources, toxicity and regulations. *Beilstein J Nanotechnol* 2018;**9**:1050-74. doi: 10.3762/bjnano.9.98.
- Johnson AC, Park B. Predicting contamination by the fuel additive cerium oxide engineered nanoparticles within the United Kingdom and the associated risks. *Environmental Toxicology and Chemistry* 2012;**31**:2582-7. doi: 10.1002/etc.1983.
- Kaegi R, Sinnet B, Zuleeg S, Hagendorfer H, Mueller E, Vonbank R, Boller M, Burkhardt M. Release of silver nanoparticles from outdoor facades. *Environmental Pollution* 2010;**158**:2900-5. doi: 10.1016/j.envpol.2010.06.009.
- Kaegi R, Ulrich A, Sinnet B, Vonbank R, Wichser A, Zuleeg S, Simmler H, Brunner S, Vonmont H, Burkhardt M, Boller M. Synthetic TiO<sub>2</sub> nanoparticle emission from exterior facades into the aquatic environment. *Environmental Pollution* 2008;**156**:233-9. doi: 10.1016/j.envpol.2008.08.004.
- Kaegi R, Voegelin A, Sinnet B, Zuleeg S, Hagendorfer H, Burkhardt M, Siegrist H. Behavior of metallic silver nanoparticles in a pilot wastewater treatment plant. *Environmental Science & Technology* 2011;**45**:3902-8. doi: 10.1021/es1041892.
- Keller AA, Lazareva A. Predicted releases of engineered nanomaterials: From global to regional to local. *Environmental Science & Technology Letters* 2014;**1**:65-70. doi: 10.1021/ez400106t.
- Keller AA, McFerran S, Lazareva A, Suh S. Global life cycle releases of engineered nanomaterials. *J Nanopart Res* 2013;**15**. doi: 10.1007/s11051-013-1692-4.
- Kinsinger N, Honda R, Keene V, Walker SL. Titanium dioxide nanoparticle removal in primary prefiltration stages of water treatment: Role of coating, natural organic matter, source water, and solution chemistry. *Environmental Engineering*

Science 2015;**32**:292-300. doi: 10.1089/ees.2014.0288.



Kiser MA, Westerhoff P, Benn T, Wang Y, Perez-Rivera J, Hristovski K. Titanium nanomaterial removal and release from wastewater treatment plants. *Environmental Science & Technology* 2009;**43**:6757-63. doi: 10.1021/es901102n.

Kreyling WG, Holzwarth U, Schleh C, Kozempel J, Wenk A, Haberl N, Hirn S, Schäffler M, Lipka J, Semmler-Behnke M, Gibson N. Quantitative biokinetics of titanium dioxide nanoparticles after oral application in rats: Part 2. *Nanotoxicology* 2017;**11**:443-53. doi: 10.1080/17435390.2017.1306893.

Lee S, Bi X, Reed RB, Ranville JF, Herckes P, Westerhoff P. Nanoparticle size detection limits by single particle ICP-MS for 40 elements. *Environmental Science & Technology* 2014;**48**:10291-300. doi: 10.1021/es502422v.

Loosli F, Wang J, Rothenberg S, Bizimis M, Winkler C, Borovinskaya O, Flamigni L, Baalousha M. Sewage spills are a major source of titanium dioxide engineered (nano)-particle release into the environment. *Environmental Science: Nano* 2019;**6**:763-77. doi: 10.1039/C8EN01376D.

Mahdi KNM, Commelin M, Peters RJB, Baartman JEM, Ritsema C, Geissen V. Transport of silver nanoparticles by runoff and erosion – A flume experiment. *Science of The Total Environment* 2017;**601-602**:1418-26. doi: <https://doi.org/10.1016/j.scitotenv.2017.06.020>.

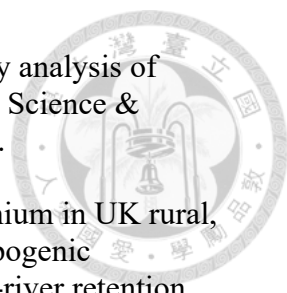
Maiga DT, Mamba BB, Msagati TAM. Distribution profile of titanium dioxide nanoparticles in South African aquatic systems. *Water Supply* 2019;**20**:516-28. doi: 10.2166/ws.2019.185.

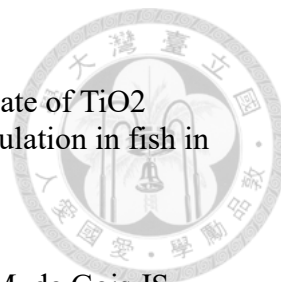
Markus AA, Krystek P, Tromp PC, Parsons JR, Roex EWM, de Voogt P, Laane RWPM. Determination of metal-based nanoparticles in the river Dommel in the Netherlands via ultrafiltration, HR-ICP-MS and SEM. *Science of the Total Environment* 2018;**631-632**:485-95. doi: 10.1016/j.scitotenv.2018.03.007.

Moon C, Park HJ, Choi YH, Park EM, Castranova V, Kang JL. Pulmonary inflammation after intraperitoneal administration of ultrafine titanium dioxide (TiO<sub>2</sub>) at rest or in lungs primed with lipopolysaccharide. *Journal of Toxicology and Environmental Health-Part a-Current Issues* 2010;**73**:396-409. doi: 10.1080/15287390903486543.

Moore MN. Do nanoparticles present ecotoxicological risks for the health of the aquatic environment? *Environment International* 2006;**32**:967-76. doi: 10.1016/j.envint.2006.06.014.

Mueller NC, Nowack B. Exposure modeling of engineered nanoparticles in the environment. *Environmental Science & Technology* 2008;**42**:4447-53. doi: 10.1021/es7029637.

- 
- Muller EB, Lin S, Nisbet RM. Quantitative adverse outcome pathway analysis of hatching in zebrafish with CuO nanoparticles. *Environmental Science & Technology* 2015;**49**:11817-24. doi: 10.1021/acs.est.5b01837.
- Neal C, Jarvie H, Rowland P, Lawler A, Sleep D, Scholefield P. Titanium in UK rural, agricultural and urban/industrial rivers: Geogenic and anthropogenic colloidal/sub-colloidal sources and the significance of within-river retention. *Science of the Total Environment* 2011;**409**:1843-53. doi: 10.1016/j.scitotenv.2010.12.021.
- Nowack B, Bucheli TD. Occurrence, behavior and effects of nanoparticles in the environment. *Environmental Pollution* 2007;**150**:5-22. doi: 10.1016/j.envpol.2007.06.006.
- Oliveira MLS, Saikia BK, da Boit K, Pinto D, Tutikian BF, Silva LFO. River dynamics and nanoparticles formation: A comprehensive study on the nanoparticle geochemistry of suspended sediments in the Magdalena River, Caribbean Industrial Area. *Journal of Cleaner Production* 2019;**213**:819-24. doi: <https://doi.org/10.1016/j.jclepro.2018.12.230>.
- Peters RJB, Oomen AG, van Bommel G, van Vliet L, Undas AK, Munniks S, Bleys RLAW, Tromp PC, Brand W, van der Lee M. Silicon dioxide and titanium dioxide particles found in human tissues. *Nanotoxicology* 2020;**14**:420-32. doi: 10.1080/17435390.2020.1718232.
- Peters RJB, van Bommel G, Milani NBL, den Hertog GCT, Undas AK, van der Lee M, Bouwmeester H. Detection of nanoparticles in Dutch surface waters. *Science of the Total Environment* 2018;**621**:210-8. doi: 10.1016/j.scitotenv.2017.11.238.
- Phalyvong K, Sivry Y, Pauwels H, Gélabert A, Tharaud M, Wille G, Bourrat X, Benedetti MF. Occurrence and origins of cerium dioxide and titanium dioxide nanoparticles in the Loire River (France) by single particle ICP-MS and FEG-SEM imaging. *Frontiers in Environmental Science* 2020. doi: <http://dx.doi.org/10.3389/fenvs.2020.00141>.
- Piccinno F, Gottschalk F, Seeger S, Nowack B. Industrial production quantities and uses of ten engineered nanomaterials in Europe and the world. *J Nanopart Res* 2012;**14**. doi: 10.1007/s11051-012-1109-9.
- Roychoudhury AN, Starke MF. Partitioning and mobility of trace metals in the Blesbokspruit: Impact assessment of dewatering of mine waters in the East Rand, South Africa. *Applied Geochemistry* 2006;**21**:1044-63. doi: <https://doi.org/10.1016/j.apgeochem.2006.02.024>.
- Sadrieh N, Wokovich AM, Gopee NV, Zheng J, Haines D, Parmiter D, Siitonen PH, Cozart CR, Patri AK, McNeil SE, Howard PC, Doub WH, Buhse LF. Lack of significant dermal penetration of titanium dioxide from sunscreen formulations containing nano- and submicron-size TiO<sub>2</sub> particles. *Toxicological Sciences* 2010;**115**:156-66. doi: 10.1093/toxsci/kfq041.



- Shi X, Li Z, Chen W, Qiang L, Xia J, Chen M, Zhu L, Alvarez PJJ. Fate of TiO<sub>2</sub> nanoparticles entering sewage treatment plants and bioaccumulation in fish in the receiving streams. *Nanoimpact* 2016;**3-4**:96-103. doi: 10.1016/j.impact.2016.09.002.
- Silva AH, Locatelli C, Filho UPR, Gomes BF, de Carvalho Junior RM, de Gois JS, Borges DLG, Creczynski-Pasa TB. Visceral fat increase and signals of inflammation in adipose tissue after administration of titanium dioxide nanoparticles in mice. *Toxicology and Industrial Health* 2017;**33**:147-58. doi: 10.1177/0748233715613224.
- Sousa VS, Teixeira MR. Removal of a mixture of metal nanoparticles from natural surface waters using traditional coagulation process. *Journal of Water Process Engineering* 2020;**36**:101285. doi: <https://doi.org/10.1016/j.jwpe.2020.101285>.
- Sun TY, Gottschalk F, Hungerbuehler K, Nowack B. Comprehensive probabilistic modelling of environmental emissions of engineered nanomaterials. *Environmental Pollution* 2014;**185**:69-76. doi: 10.1016/j.envpol.2013.10.004.
- Tiede K, Hanssen SF, Westerhoff P, Fern GJ, Hankin SM, Aitken RJ, Chaudhry Q, Boxall ABA. How important is drinking water exposure for the risks of engineered nanoparticles to consumers? *Nanotoxicology* 2016;**10**:102-10. doi: 10.3109/17435390.2015.1022888.
- Ullmann C, Babick F, Stintz M. Microfiltration of submicron-sized and nano-sized suspensions for particle size determination by dynamic light scattering. *Nanomaterials (Basel)* 2019;**9**:829. doi: 10.3390/nano9060829.
- van Ravenzwaay B, Landsiedel R, Fabian E, Burkhardt S, Strauss V, Ma-Hock L. Comparing fate and effects of three particles of different surface properties: Nano-TiO<sub>2</sub>, pigmentary TiO<sub>2</sub> and quartz. *Toxicology Letters* 2009;**186**:152-9. doi: <https://doi.org/10.1016/j.toxlet.2008.11.020>.
- Velzeboer I, Quik JT, van de Meent D, Koelmans AA. Rapid settling of nanoparticles due to heteroaggregation with suspended sediment. *Environ Toxicol Chem* 2014;**33**:1766-73. doi: 10.1002/etc.2611.
- Venkatesan AK, Reed RB, Lee S, Bi X, Hanigan D, Yang Y, Ranville JF, Herckes P, Westerhoff P. Detection and Sizing of Ti-containing particles in recreational waters using single particle ICP-MS. *Bulletin of Environmental Contamination and Toxicology* 2018;**100**:120-6. doi: 10.1007/s00128-017-2216-1.
- Veselý J, Majer Vr, Kučera J, Havránek Vr. Solid–water partitioning of elements in Czech freshwaters. *Applied Geochemistry* 2001;**16**:437-50. doi: [https://doi.org/10.1016/S0883-2927\(00\)00041-X](https://doi.org/10.1016/S0883-2927(00)00041-X).
- von Moos N, Slaveykova VI. Oxidative stress induced by inorganic nanoparticles in bacteria and aquatic microalgae - state of the art and knowledge gaps.

Nanotoxicology 2014;**8**:605-30. doi: 10.3109/17435390.2013.809810.

Wang J, Nabi MM, Mohanty SK, Afrooz ARMN, Cantando E, Aich N, Baalousha M. Detection and quantification of engineered particles in urban runoff. *Chemosphere* 2020;**248**:126070. doi: <https://doi.org/10.1016/j.chemosphere.2020.126070>.

Wang J, Zhou G, Chen C, Yu H, Wang T, Ma Y, Jia G, Gao Y, Li B, Sun J, Li Y, Jiao F, Zhao Y, Chai Z. Acute toxicity and biodistribution of different sized titanium dioxide particles in mice after oral administration. *Toxicology Letters* 2007;**168**:176-85. doi: 10.1016/j.toxlet.2006.12.001.

Warheit DB, Donner EM. Risk assessment strategies for nanoscale and fine-sized titanium dioxide particles: Recognizing hazard and exposure issues. *Food and Chemical Toxicology* 2015;**85**:138-47. doi: <https://doi.org/10.1016/j.fct.2015.07.001>.

Weir A, Westerhoff P, Fabricius L, Hristovski K, von Goetz N. Titanium dioxide nanoparticles in food and personal care products. *Environmental Science & Technology* 2012;**46**:2242-50. doi: 10.1021/es204168d.

Westerhoff P, Atkinson A, Fortner J, Wong MS, Zimmerman J, Gardea-Torresdey J, Ranville J, Herckes P. Low risk posed by engineered and incidental nanoparticles in drinking water. *Nature Nanotechnology* 2018;**13**:661-9. doi: 10.1038/s41565-018-0217-9.

Westerhoff P, Song G, Hristovski K, Kiser MA. Occurrence and removal of titanium at full scale wastewater treatment plants: implications for TiO<sub>2</sub> nanomaterials. *Journal of Environmental Monitoring* 2011;**13**:1195-203. doi: 10.1039/c1em10017c.

Yang Y, Long CL, Li HP, Wang Q, Yang ZG. Analysis of silver and gold nanoparticles in environmental water using single particle-inductively coupled plasma-mass spectrometry. *Science of the Total Environment* 2016;**563**:996-1007. doi: 10.1016/j.scitotenv.2015.12.150.

Yang Y, Westerhoff P. Presence in, and release of, nanomaterials from consumer products. In: Capco DG, Chen Y, eds. *Nanomaterial: Impacts on Cell Biology and Medicine* 2014;1-17.

Zhang C, Fan Y, Wang X, Xing X, Chen X, Zhang J, Bian J. Bench-scale Study on the removal of TiO<sub>2</sub> nanoparticles in natural lake water by coagulation. *Chemistry Letters* 2017;**46**:1846-8. doi: 10.1246/cl.170852.

林柏青、衛紀淮、何良勝：102 年港域近岸底床輸砂之現場觀測研究 (1/4)。初版。台灣：交通部運輸研究所，2014；109-110。

陳正宏：臺灣地質系列第 1 號：臺灣之火成岩。初版。臺北縣中和市：經濟部中

央地質調查所，1990；68-69。

國立臺灣大學公共衛生學院健康風險及政策評估中心 (2008)：台灣一般民眾暴露參數彙編。行政院衛生署委託計畫。計畫編號：DOH96-HP-1801。台北：行政院衛生署。

經濟部水利署。水文資訊網整合服務系統。Available at:

<https://gweb.wra.gov.tw/Hydroinfo/?id=Index>. Accessed August 5, 2020.

鍾季桓。環境水體及淨水流程中二氧化鈦奈米微粒濃度及粒徑分佈先驅研究。國立台灣大學碩士論文。2019，45p。

